

Research and Development



# Optical Detection of Fiber Particles in Water



## RESEARCH REPORTING SERIES

Research reports of the Office of Research and Development, U.S. Environmental Protection Agency, have been grouped into nine series. These nine broad categories were established to facilitate further development and application of environmental technology. Elimination of traditional grouping was consciously planned to foster technology transfer and a maximum interface in related fields. The nine series are:

1. Environmental Health Effects Research
2. Environmental Protection Technology
3. Ecological Research
4. Environmental Monitoring
5. Socioeconomic Environmental Studies
6. Scientific and Technical Assessment Reports (STAR)
7. Interagency Energy-Environment Research and Development
8. "Special" Reports
9. Miscellaneous Reports

This report has been assigned to the ENVIRONMENTAL PROTECTION TECHNOLOGY series. This series describes research performed to develop and demonstrate instrumentation, equipment, and methodology to repair or prevent environmental degradation from point and non-point sources of pollution. This work provides the new or improved technology required for the control and treatment of pollution sources to meet environmental quality standards.

EPA-600/2-79-127  
August 1979

OPTICAL DETECTION OF FIBER PARTICLES IN WATER

by

S. R. Diehl, D. T. Smith, M. Sydor  
Department of Physics  
University of Minnesota, Duluth  
Duluth, Minnesota 55812

Grant No. R804361-02-0

Project Officer

Gary S. Logsdon  
Drinking Water Research Division  
Municipal Environmental Research Laboratory  
Cincinnati, Ohio 45268

MUNICIPAL ENVIRONMENTAL RESEARCH LABORATORY  
OFFICE OF RESEARCH AND DEVELOPMENT  
U.S. ENVIRONMENTAL PROTECTION AGENCY  
CINCINNATI, OHIO 45268

## DISCLAIMER

This report has been reviewed by the Municipal Environmental Research Laboratory, U.S. Environmental Protection Agency, and approved for publication. Approval does not signify that the contents necessarily reflect the views and policies of the U.S. Environmental Protection Agency, nor does mention of trade names or commercial products constitute endorsement or recommendation for use.

## FOREWORD

The Environmental Protection Agency was created because of increasing public and government concern about the dangers of pollution to the health and welfare of the American people. Noxious air, foul water, and spoiled land are tragic testimony to the deterioration of our natural environment. The complexity of that environment and the interplay between its components require a concentrated and integrated attack on the problem.

Research and development is that necessary first step in problem solution and it involves defining the problem, measuring its impact, and searching for solutions. The Municipal Environmental Research Laboratory develops new and improved technology and systems for the prevention, treatment, and management of wastewater and solid and hazardous waste pollutant discharges from municipal and community sources, for the preservation and treatment of public drinking water supplies, and to minimize the adverse economic, social, health, and aesthetic effects of pollution. This publication is one of the products of that research; a most vital communications link between the researcher and the user community.

Water filtration for asbestiform fiber removal has been studied at Duluth, Minnesota and Seattle, Washington, and a 30 million gallon per day plant has been built and is operating at Duluth. This report describes research to develop a rapid means of detecting fibers in water so that the quality of potable water can be monitored as it is actually being produced, in contrast to days or weeks of delay necessary for electron microscope analysis.

Francis T. Mayo, Director  
Municipal Environmental Research  
Laboratory

## ABSTRACT

Light scattering by individual particulates is used in a multiple-detector system to categorize the composition of suspended solids in terms of broad particulate categories. The scattering signatures of red clay and taconite tailings, the two primary particulate contaminants in western Lake Superior, along with two types of asbestiform fibers, amphibole, and chrysotile, were studied in detail. A method was developed to predict the concentration of asbestiform fibers in filtration plant samples for which electron microscope analysis was done concurrently. Fiber levels as low as  $5 \times 10^4$  fibers/liter were optically detectable. The method offers a fast and inexpensive means for measuring, either on a continuous basis or as discrete samples, the fiber levels of filtration plant output. Further calibration of the instrument could enable analysis for other specific particulate contaminants as well.

This report was submitted in fulfillment of Grant No. R804361-02-0 by the University of Minnesota, Duluth Department of Physics under the sponsorship of the U.S. Environmental Protection Agency. This report covers the period March 8, 1976 to September 7, 1978, and work was completed as of May 16, 1978.

## CONTENTS

Foreword . . . . .	iii
Abstract . . . . .	iv
Figures . . . . .	vi
Tables . . . . .	vii
Abbreviations and Symbols . . . . .	viii
Acknowledgment . . . . .	ix
1. Introduction . . . . .	1
2. Conclusion . . . . .	3
3. Recommendations . . . . .	4
4. Apparatus . . . . .	6
5. Analysis Method . . . . .	7
6. Results . . . . .	9
Individual particle types . . . . .	9
Predicting concentrations . . . . .	12
7. Application to Samples Containing Fibers . . . . .	14
8. Refinements to the Apparatus . . . . .	21
References . . . . .	48
Appendix . . . . .	50

## FIGURES

<u>Number</u>		<u>Page</u>
1	Size distribution of fibers found in Duluth drinking water . . . . .	24
2	Block diagram of apparatus . . . . .	25
3	Number of events at the $\pm 45^\circ$ detector pair versus concentra- tion for each particle type . . . . .	26
4	Region assignments for the $\pm 45^\circ$ detectors . . . . .	27
5	Region assignments for the $\pm 90^\circ$ detectors . . . . .	28
6	Region assignments for the $+ 45^\circ$ and $+ 135^\circ$ detectors . . . . .	29
7	Region assignments for the $+ 45^\circ$ and $- 135^\circ$ detectors . . . . .	30
8	Percent of total counts versus counting region at $\pm 45^\circ$ for each particle type . . . . .	31
9	Percent of total counts versus counting region at $\pm 90^\circ$ for each particle type . . . . .	32
10	Percent of total counts versus counting region at $+ 45^\circ$ , $- 135^\circ$ for each particle type . . . . .	33
11	Percent of total counts versus counting region at $+ 45^\circ$ , $+ 135^\circ$ for each particle type . . . . .	35
12	Predicted versus measured total fibers for Duluth water samples and $\pm 45^\circ$ scattering angles . . . . .	37
13	Total counts at $\pm 45^\circ$ versus EM total fiber concentrations . . . . .	38
14	Predicted versus measured total fibers for Duluth water and $\pm 90^\circ$ scattering angles . . . . .	39
15	Predicted versus measured total fibers for Duluth water and $+ 45^\circ$ , $- 135^\circ$ scattering angles . . . . .	40
16	Predicted versus measured total fibers for Duluth water and $+ 45^\circ$ , $+ 135^\circ$ scattering angles . . . . .	41
17	Predicted versus measured total fibers for Seattle raw water . . . . .	42
18	Predicted versus measured total fibers for Seattle finished water . . . . .	43
19	Comparison of predicted total fibers and EM measurements for data collected using the modified apparatus . . . . .	44
20	Prediction of amphibole fibers versus the EM measurements for the modified apparatus . . . . .	45
21	Particle counter data versus EM amphibole fiber counts . . . . .	46
22	Particle counts versus EM total fiber counts . . . . .	47



## TABLES

<u>Number</u>		<u>Page</u>
1	Coefficients of for the $\pm 45^\circ$ fit to Duluth filtered water . . . .	16
2	Coefficients for $\pm 90^\circ$ fit . . . . .	17
3	Coefficients for the $+ 45^\circ$ , $- 135^\circ$ fit . . . . .	18
4	Coefficients for the $+ 45^\circ$ , $+ 135^\circ$ fit . . . . .	18
5	Coefficients for the fit to Seattle raw water. . . . .	20
6	Coefficients for the fit to Seattle filter water . . . . .	20

## LIST OF ABBREVIATIONS

ADC	-- analog to digital converter
A/D	-- analog to digital
C	-- coincident
EM	-- electron microscope
Hz	-- hertz
mm	-- millimeter
N	-- non-coincident
SAD	-- selected area diffraction
sec	-- second
$\mu\text{m}$	-- micrometer
$\mu\text{g}$	-- microgram
$\mu\text{g}/\ell$	-- microgram per liter
$^{\circ}\text{C}$	-- degree centigrade

## ACKNOWLEDGMENTS

We would like to offer our sincere thanks to the personnel at the Duluth Filter plant for their cooperation. We are also especially grateful to the people of the Lake Superior Basin Studies Center who were involved with the collection of the electron microscope data. Their dedication and assistance were greatly appreciated.

## SECTION 1

### INTRODUCTION

Over the past several years the presence of fibrous asbestiform particulates has been observed in a number of municipal water supplies throughout the U.S. The possible health hazard which these fibers present has spurred a great deal of interest in the problems of detection and removal of the submicroscopic particulates in water. While the removal of amphibole-asbestos has reached a high state of the art in the Duluth, Minnesota filtration plant, advanced detection techniques have been slow in developing and investigators have been forced to rely on tedious and time consuming methods.

Electron microscopy and x-ray diffraction techniques are the most widely used in the detection of asbestiform fibers. Both techniques require expensive equipment, tedious sample preparation, and have other severe limitations. X-ray diffraction has a very low detection sensitivity ( $\sim 10 \mu\text{g}$ )<sup>1,2</sup> and requires a relatively large amount of asbestiform material, thus necessitating filtration of a very large volume sample, (over 50 liters has been needed for some clean samples). Filtration of large volume samples creates problems since the filters often become completely plugged with suspended material, such as the aluminum hydroxide present in filter plant effluent, making the collection of enough asbestos material for analysis impossible.

Electron microscopy has good sensitivity ( $0.1 \mu\text{g}$  has been claimed)<sup>3</sup> but is both costly and time consuming requiring from several hours to two days for one sample analysis. Electron microscope results are also highly dependent upon the method of sample preparation and interpretation by the observer doing the actual counting. Thus repeatability is poor and the error for a particular low-concentration sample can be very high.<sup>4</sup>

The purpose of this paper is to introduce a new technique for the detection of submicroscopic fibers which is fast, inexpensive, and has demonstrated high repeatability. The method employs single-particle scattering in which a focused laser beam passing through a liquid sample illuminates single particles at the focal point of a system of detectors. The signal received at the detectors is recorded sequentially for each particle drifting through the focal point. At the end of the test the data are analyzed for particle type and particle concentration. Thus far, the primary purpose has been to detect rod-like particles and the data has been correlated only to fibrous particles, but other particle symmetries can be discerned with proper calibration procedures.

The scattering of electromagnetic waves by dielectric objects has received much attention over the years. The fundamental theory was given by Lord Rayleigh in 1871<sup>5</sup> and has been extended by many others since then. The theory is straight-forward for the cases in which the scattering bodies are very small (Rayleigh Scattering), or very large (geometrical optics) compared to the wavelength of the incident radiation. However, the mathematics for the so-called "resonance region," in which particle dimensions are of the same magnitude as the wavelength, is complex. In this region the complete wave nature of the incident radiation must be considered. While early solutions to the scattering problem were found for spheres in three dimensions, (Mie theory)<sup>6,7</sup> and infinite circular cylinders<sup>6,7,8</sup> in two dimensions, only recently have solutions been obtained for arbitrarily shaped bodies including finite circular cylinders.

Work by Barber and Yeh<sup>9</sup> as well as that by Birkhoff et al.<sup>10</sup> has shown that the scattered radiation from rod-like particles is dependent upon the angle of incidence to the radiation field. Mie theory demonstrates that the radiation pattern of spherical particles depends only upon particle size and index of refraction and has complete symmetry about the optical axis. Observing the symmetry of the scattered light of single particles in a monochromatic beam should thus allow for the discrimination of needle-like particles from a mass of other particles in a sample.

The problem is complicated by the fact that the actual radiation patterns for both spheres and cylinders show many maxima and minima. The books by Van de Hulst<sup>6</sup> and Born and Wolf<sup>11</sup> give radiation patterns for spheres in the resonance region. Patterns for cylinders in various orientations can be found in the works by Barber and Yeh<sup>9</sup>, Farone and Kerker<sup>12</sup>, and Kerker, Cooke, Farone, and Jacobsen<sup>13</sup>. Particles of other than spherical or cylindrical symmetry (e.g. ellipsoids) also show characteristic multiple-lobe radiation patterns<sup>9</sup>.

Asbestos fibers occurring in the environment are commonly of a size which places them within the resonance region of visible light (Figure 1). Thus the detection of these particles cannot be carried out by commonly available instruments using volume reflectance measurements based upon Mie or Rayleigh scattering. Furthermore, volume scattering has been shown to be of limited usefulness for the detection of particles which lack characteristics that produce a volume interference effect<sup>14,15</sup>. Identification should be possible, however, by observations of the symmetry of the scattered light from individual particles. However, the problem is complicated by the fact that the fibers exist in a medium containing many other particles of varying shapes and sizes. It is thus necessary to find a scattering signal unique to needle-like particles amid a great deal of background "noise" due to other suspended particles.

To this end an instrument has been designed using multiple detectors to monitor the symmetry of the scattered light due to single particles in a laser beam. Comparison of the scattering signal to electron microscope fiber counts for each sample allowed the extraction of the fiber signature from the background noise.

## SECTION 2

### CONCLUSION

The multiple-detector scattering method has shown itself to be of considerable value for the measurement of fiber concentrations in water. If calibrated with a sufficient amount of EM data, the method actually yields results which are more accurate than a single standard EM fiber analysis. Furthermore, it seems likely that any particle type whose size is on the same order of magnitude as the wavelength of the incident beam could be distinguished from a background of other particulates. They need only to differ in shape or the index of refraction. However, routine calibration checks should be made and the calibration criteria should be updated as additional data becomes available. Checks on irregularities of filtered product could also be built in.

Once completely programmed, the microcomputer will make the apparatus portable and extremely easy to operate. After answering a few questions from the keyboard about such things as the desired test duration, the operator must only wait for the concentrations to be displayed. If needed, the apparatus could be modified to function as an on-line monitoring device with the most recent fiber concentrations continually displayed. In fact, the increased rate at which the particles would be carried through the beam in a flow-through system would mean an increase in the accuracy of the measurements for a given test duration.

## SECTION 3

### RECOMMENDATIONS

An optical method for the detection of fibers in water has been constructed to provide a capability for checking the effectiveness of filtration processes for removing fibers. The method differs from a turbidity meter in that it provides not only the information on total turbidity as does an ordinary turbidity meter or particle counter, but also provides information on the actual fiber count. Thus, even if the total turbidity remains relatively steady but the fiber removal process is not working properly, the instrument would sound a warning within several minutes. This feature is quite essential in monitoring plants where most of the turbidity is due to particulates other than the fibers.

The instrument works on the principle of optical categorization of turbidity samples particle by particle. In this method particulates are identified by their light scattering envelope. A particle illuminated by a beam of light scatters photons in various directions with intensities which depend on particle size, its shape, its relative index of refraction, and its orientation in the beam. The scattered light envelope is thus characteristic of the physical properties of the particle. In this apparatus individual particles drifting through a tiny volume of space are viewed simultaneously by several detectors. The set of signals from the detectors are fed into a microprocessor-computer which automatically identifies the set of simultaneous pulses as those belonging to a scattering envelope characteristic of a certain species of particulates. Thus, by counting the abundance of various species of particulates we can determine the composition of the suspended solids on a statistical basis. In the case of monitoring a filtration plant output the instrument can be programmed to record only the concentrations of fibers and the total particulate count. The system is calibrated for detection of a specific particulate category, by using electron microscopy data for that species in conjunction with scattering information. The instrument remains in calibration provided no new major species of particulates is introduced into the background and the optical surfaces remain aligned and clean. Thus, one would anticipate, for maintenance purposes, a monthly check on the optics and a semiannual check on calibration.

The present system is a bench type instrument but the method should be modified and applied to an on-line operation where it could greatly improve the monitoring of the fiber removal process. The basic components and rough costs for a system are: light source (\$2,000), circuitry and detectors (\$1,000), machining of chamber and detector mountings (\$3,000), and

microprocessor and programs (\$4,000). The cost of calibration would be around \$8,000 plus the cost of electron microscope data.

The system can be constructed to require minimal operator skill to read out fiber count and perform routine tests on the operation of the system. The entire method can be reduced to simple push button operation. Actually, for reasonably skilled operators, the instrument is flexible enough to provide a facility for testing of plant operation efficiency and for data compilation and recording.



## SECTION 4

### APPARATUS

The schematic for the apparatus is shown in Figure 2. A laser beam which is focused to a diameter of .1 mm passes through a water sample containing suspended particles. Six photodiode detectors are mounted around the sample at the angles  $\pm 45^\circ$ ,  $\pm 90^\circ$ , and  $\pm 135^\circ$  to the incident beam. As individual particles drift through the beam, the resulting scattered light produces, at each detector output, signals which appear as a series of pulses of various sizes and shapes with an average width of about .2 - .3 seconds.

A lens in conjunction with a narrow aperture increases the light gathering ability of each photodiode and yet limits the length of the beam viewed by the detectors to 1 mm. This, together with the narrow beam diameter, ensures, for low concentration samples, that only single-particle events are viewed by the detectors at any time. In addition, since each lens subtends an angle of about  $10^\circ$ , all the light scattered in a cone toward the lens is detected by the photodiode producing an integrated signal which smooths out the narrow angular fluctuation of the scattered light.

An analog to digital converter was designed to simultaneously sample any two of the six detectors at a 15 Hz rate (by integrating for 1/15 second), and transmit the data by telephone directly to the university computer where it was stored for future analysis. A higher sampling rate was not possible due to the fixed transmission rate of the computer phone link. To observe adequately the characteristics of the scattering signal, a two channel digital storage device was used to sample and display a 5 or 10 second time segment of the two detector output.

## SECTION 5

### ANALYSIS METHOD

In considering the scattered signal by examining simultaneous pulse heights for the six detectors many sampling schemes were possible. Three pairs of viewing angles were initially chosen:  $\pm 45^\circ$ ,  $\pm 90^\circ$ , and  $\pm 45^\circ$  with  $-135^\circ$ . A fourth combination at  $+45^\circ$  and  $+135^\circ$  was added later. The polarization plane of the laser beam was always held perpendicular (vertical) to the plane of the detectors. The parallel case was also examined but was not considered in detail.

To measure accurately the concentrations of unknown samples, the number of events seen per unit of time for any given sample should remain constant and should be proportional to the concentration of particulates. It was found, however, that weak convection currents caused by the difference in temperature between the sample and its surroundings were able to influence the rate at which particles drift through the beam. In fact, the event rate for a typical sample chilled to near  $0^\circ\text{C}$  prior to testing, slowly dropped over an 8 hour period to about one-fourth of its starting value. After 24 hours with the sample near equilibrium, particles would cease to travel directly through the beam and would on occasion appear to rotate or move repeatedly in and out of the beam.

The following test procedure was thus implemented to improve repeatability and to obtain a high event rate:

- 1) The sample was first refrigerated at near  $0^\circ\text{C}$  for at least 12 hours.
- 2) One hour prior to testing, the sample was vigorously agitated to thoroughly resuspend the particles and then again refrigerated to allow bubbles to dissipate.
- 3) The sample was removed from refrigeration one-half hour prior to testing.
- 4) Ten minutes prior to testing, the sample was gently agitated to resuspend any settled particles and placed in the scattering chamber.
- 5) Using the A/D converter, ten minutes of detector data was sent to the computer for each angle pair.

Once data files were created for a sample, all the advantages and options of the computer were available for data analysis. A program was written which first searched each digitized detector output for a repetitive minimum, i.e. baseline, to use for the detector zeros. The program then

searched the data for peaks. Once a peak was located, its height and the level of the signal in the accompanying detector were stored in memory. However, only events which exceeded a predefined cutoff set sufficiently above the noise level were stored. If the accompanying detector also produced a peak, i.e. if the peaks occurred simultaneously, the zero-corrected peak heights were stored together and labeled as a "coincident" pair. Otherwise, the event for a given detector was labeled as non-coincident. In order to reduce the uncertainty between the measured and actual peak heights due to the finite sampling rate, the stored value for the peak height was averaged over the adjacent digital sampling times.

## SECTION 6

### RESULTS

#### INDIVIDUAL PARTICLE TYPES

Files for the peak heights and the corresponding coincidence information were created from the original digitized data for a variety of different particle types. Amosite, red clay, and taconite tailings in two size ranges,  $< 2 \mu\text{m}$  and  $2 - 5 \mu\text{m}$ , were studied. Information on spherical scatterers was provided by data from  $.6$  and  $1.1 \mu\text{m}$  uniform latex spheres. Canadian chrysotile with an average fiber length of  $2 - 3 \mu\text{m}$  was also investigated. Four concentrations of each sample type were tested as a check on linearity and our dilution techniques, and each sample was run at least twice as a check on repeatability.

A plot of the total number of events at the  $\pm 45^\circ$  detector pair versus concentration can be seen in Figure 3 for the smaller particle size range. Each sample counting rate was corrected for background by also testing the water used for sample dilution. The counting rate from background water was subtracted from the counting rates for the samples. The plotted points in Figure 3 appear quite linear, and the small deviations from the straight-line fits could easily arise from any number of factors including sample contamination or sample dilution errors which are always possible at such low concentrations. For the  $< 2 \mu\text{m}$  range at higher concentrations, the maximum spread in the total number of events changed less than 5% after repeated testing with the  $\pm 45^\circ$  detector pair. The spread was less than 10% for the other three detector pairs. The lower gain and the improved zero stability of the  $\pm 45^\circ$  detector configuration may account for this difference. Fluctuations in the number of events were a little more noticeable for the larger particle sizes. In such cases changes in particle settling rates become noticeable even with small deviations in the test procedure.

Distribution plots for both the coincident and non-coincident events can be found in the appendix for each of the particle types. Only the  $\pm 45^\circ$  and the  $+ 45^\circ$  with  $- 135^\circ$  detector pairs are shown in detail. The results for the  $\pm 90^\circ$  and  $+ 45^\circ$  with  $+ 135^\circ$  pairs are similar. The  $\pm 45^\circ$  data were categorized by sorting the events into a  $21 \times 26$  element array on a plot representing maximum pulse height along one axis and pulse ratio along the other. The pulse ratios for coincident events were obtained by dividing the smaller of the two peaks by the larger to give ratios always less than one. For the non-coincident events the ratio value was taken as the level of the detector at which no pulse occurred divided by the peak height found at the opposite detector. Because of the symmetry of the  $\pm 45^\circ$  detectors, no

information is lost by plotting ratios in this fashion, but instead, the number of events of a given ratio are in effect doubled. It was hoped that the pulse ratios would tend to be independent of particle size but dependent on particle type.

For the distribution plots with the detectors at  $+45^\circ$  and  $-135^\circ$ , the events were sorted into an array either by peak height versus peak height in the case of coincident events or by peak height versus the level of the opposite detector for the non-coincident events. Because of the lack of symmetry of the  $+45^\circ$  and  $-135^\circ$  detector pair with respect to the beam, the non-coincident events were categorized separately for the  $+45^\circ$  from those which occurred at the  $-135^\circ$  detector.

All the samples of each particle type were combined to reduce statistical fluctuations between adjacent array elements. The distributions were background corrected by smoothing both the sample array and the background array and then subtracting the corresponding array elements. (The smoothing was done in a manner which conserved the total number of events and allowed a change of at most four events per array element.) To compare between particle types, the arrays were normalized by dividing the number of events in each element of an array by the total number of events. Thus each contour line on the pulse height versus pulse ratio array represents a line of equal event probability given in percent. To avoid the loss of data, whenever a large peak went off scale, the event was summed into a location at the array boundaries. This accounts for the concentration of contour lines seen near the boundaries of the arrays, particularly for the runs representing the larger particle types. For the  $\pm 45^\circ$  non-coincident case, events with ratios larger than 1.0 were summed into the edge array locations. The contour lines are also artificially compacted near the lower boundaries because of the cutoff level.

The distribution plots for the  $.6\text{ }\mu\text{m}$  latex spheres reveal a number of peculiarities of the equipment and the method. Due to spherical symmetry of the latex particles, light should scatter symmetrically about the beam in the plane of the detectors. Thus one would expect for the  $\pm 45^\circ$  detector pair that all of the events would fall in the coincident plot and have ratios of exactly one. Obviously, this is not exactly the case. Although most of the events did bunch up on the coincident distribution plot near the 1.0 ratio boundary, about 25% of the events fell in the non-coincident plot. One explanation for this is that the detectors are slightly out of alignment, and consequently, the lengths of the beam viewed by each detector do not completely overlap. An occasional particle could be seen by one detector and not the other, which would primarily account for the events with low ratios.

The remainder of the non-coincident events, however, result from the interaction of the low A/D converter resolution with the cutoff level. Due to the  $\pm 1$  bit out of 7 bit (1.5% of full scale) accuracy of the A/D converter, it is possible for a pulse to just exceed the cutoff level of one detector but not the other. Such an event would thus be defined as non-coincident. This is especially noticeable for  $+45^\circ$  and  $-135^\circ$  detectors where the light scattered by the  $.6\text{ }\mu\text{m}$  latex spheres seldom if ever exceeded

the - 135° detector cutoff and most of the events were labeled as non-coincident.

The apparent concentration of events on the  $\pm 45^\circ$  plots at a few particular ratios is also caused by the finite step size of the A/D converter. At low peak heights the ratios begin to take on noticeably discrete values due to the division of one small integer value by another. It should be noted here that the Gaussian-shaped beam intensity and slow sampling rate also produced a significant spread in the measured peak heights, despite the uniformity of the latex spheres. But since such deviations from the mean peak height are the same at both detectors, the ratios should be unaffected.

To make quantitative measurements of the amounts of various types of suspended solids found in an unknown sample, it is necessary that each particle type must have its own scattering signature. Aside from the more obvious differences due to particle size, however, the pulse height and pulse ratio distribution plots for the various particle types, excluding the latex spheres, all have a somewhat similar pattern. This is not surprising when one considers the asymmetric nature of such particles. For example, under the electron microscope, many red clay particles appear as elliptical platelets which could at least in some orientations scatter light in a fashion similar to the fibers found in the amosite and chrysotile samples. The wide variation in particle size and shape found even in just one general particle type also tends to wash out any characteristic features of the scattered light.

However, significant differences do exist. The  $\pm 45^\circ$  distribution plots for  $< 2 \mu\text{m}$  red clay have nearly twice the number of coincident events with ratios near 1.0 than does any of the other particle types. This simply suggests that the smaller red clay particles tend to be more spherically symmetric. Comparing the red clay ( $< 2 \mu\text{m}$ ) and tailings ( $< 2 \mu\text{m}$ ) contour plots to the plots for amosite ( $< 2 \mu\text{m}$ ) and chrysotile for the  $\pm 45^\circ$  non-coincident distributions, one observes a shift in amosite and chrysotile toward low pulse-height ratios. The samples of larger particle size (2 - 5  $\mu\text{m}$ ) also showed pronounced differences; amosite produced more high-intensity off-scale coincident events than did red clay even though red clay generated more events with intermediate peak heights. Some of the contour plots also revealed a few pronounced maxima. Chrysotile, for instance, has a build-up of non-coincident events at the ratios of .2 and .5 on the  $\pm 45^\circ$  detector pair plots.

Similar differences exist for the + 45° and - 135° detector pair. Red clay again had the highest percentage of coincident events with small peak heights. On the - 135° non-coincident plot, chrysotile produced a maximum in the number of events which is over four times higher than the same region for other event distributions. The association of fibrous material, spheres, and block particles with certain regions on the pulse height and pulse ratio plots provide a means of categorizing the signals in unknown samples into fibrous and nonfibrous particle types, and a means for predicting particle type concentrations.

## PREDICTING CONCENTRATIONS

Since the event distributions showed significant differences for particle types, it should be possible to make quantitative predictions about the concentration of an individual particle type in a sample. Consider subdividing the event distribution plots of an unknown sample into  $n$  smaller regions. In any given region the event rate, i.e. the number of events per unit time, should be proportional to the concentrations of the various particle types. Thus, for all of the  $n$  regions one has a system of equations of the form:

$$\begin{aligned} N_1 &= a_1 C_1 + b_1 C_2 + c_1 C_3 + \dots \\ N_2 &= a_2 C_1 + b_2 C_2 + c_2 C_3 + \dots \\ &\vdots \\ N_n &= a_n C_1 + b_n C_2 + c_n C_3 + \dots \end{aligned} \quad (1)$$

where  $N_1, N_2, \dots, N_n$  = the event rate in each region,

$C_1, C_2, C_3, \dots$  = the unknown concentrations of various types of suspended solids,

and  $a_1, b_1, c_1, \dots$  = the coefficients of proportionality.

Provided the subdivision of the pulse height-pulse ratio distribution incorporates a sufficient number of regions to identify all major particulate types and provided the resulting system of  $n$  simultaneous equations is linearly independent, one may solve for each of the unknown concentrations.

For example, the equation for  $C_1$  is given by

$$C_1 = a_1' N_1 + b_1' N_2 + c_1' N_3 + \dots + d_1' N_n \quad (2)$$

where  $a_1', b_1', c_1', d_1', \dots$  are functions of the original  $a$ 's,  $b$ 's,  $c$ 's,  $d$ 's,  $\dots$  etc. So each unknown concentration can simply be expressed as a linear sum of the event rates of the  $n$  regions.

In practice it is desirable to keep the number of unknowns to a minimum, i.e. group the categories of particles which are not of interest into broader regions. Unfortunately, it may be necessary to subdivide a classification of a specific category of particles if the constituents vary independently from sample to sample. For example, particles labeled as "fibers" may have to be grouped by type or perhaps even length. To obtain total fibers, however, one just sums the individual equations which again results in a linear sum of the  $n$  region event rates, but with different coefficients.

Solving for the necessary coefficients by experimenting with each individual particle type which is present in an unknown sample would usually be impractical, especially if one is only interested in the level of some specific contaminant. In fact, it may not be possible to isolate or identify some of the background particulates. One approach is to test samples which contain various known amounts of the particle type that one desires to identify and an independently varying amount of other background particulates. Linear-regression analysis can then be used to find the set of coefficients which gives a least-square fit to the measured concentrations of the known particle type. The number and the manner of subdivision of the pulse height regions chosen can be altered until a satisfactory fit is obtained. It should be pointed out, however, that if one uses as many variables, i.e. regions, as there are test samples, the linear regression will produce an exact fit independent of the actual number of particle types. Therefore to obtain a statically valid fit, the number of test samples should be at least several times larger than the final number of variables.



## SECTION 7

### APPLICATION TO SAMPLES CONTAINING FIBERS

During a six month period, over 60 Duluth and 30 Seattle water samples were tested for which electron microscope (EM) data was available. All of the Duluth samples were filter effluent from either the main plant which supplies Duluth tap water or from an adjoining pilot plant operation. The Seattle samples consisted of both pilot plant, filter effluent and raw intake water. Since the samples contained measured concentrations of fibers, including both amphibole and chrysotile asbestos, they presented an ideal opportunity to directly test and improve the scattering method for the detection of fibers in water.

Prior to analyzing the filtration plant data, the pulse height distribution plots for each detector pair were subdivided into 12 regions in a manner which accented the differences seen between the various test samples of the known particle types: amosite, chrysotile, red clay, tailings, and spheres. This yielded pulse height ratio regions which would differentiate at least the tested particle types and possibly others. The choices for each of the four detector pairs are depicted in Figures 4 - 7. Figures 8 - 11 show the percentage of event types found in each region for the particle types tested and for the Duluth and Seattle samples. The unique signatures for various particulates is apparent at all four of the detector pairs.

Since the EM analysis for the Duluth and Seattle samples was performed by independent laboratories using different techniques, the two sets of data were handled separately. Otherwise, sources of error which vary from one EM analysis to the other would make correlation of the optical data to EM data difficult. If the data for Duluth and Seattle samples were to be combined, the presence of different background particulates and different types and sizes of fibers would also necessitate a large number of fitting variables, complicating the interpretation of the results.

The primary fiber of interest in the Duluth water is amphibole asbestos, although chrysotile fibers are also present in smaller amounts. The Duluth EM data which we received included the counting of amphibole and chrysotile fibers that were positively identified using selected-area diffraction (SAD). Other fibers were also counted provided they had the correct morphology, such as nearly parallel sides, even though no SAD patterns were observed or the patterns were ambiguous. (The usual 3:1 aspect ratio was used to define the cutoff between fibers and non-fibers.) The total number of fibers that were recorded per sample was usually less than 20, of which only a few were positively identified as amphibole or chrysotile. As pointed out by

Leineweber<sup>4</sup>, the statistical uncertainty for such low numbers of fibers is extremely high, and the resulting spread in the data makes it difficult to evaluate the quality of the mathematical fits. To improve the situation, the lower concentration samples were grouped by their number of observed fibers and averaged. This tends to smear out any sample to sample variations which might occur. Even with sample averaging, the number of positively-identified amphibole or chrysotile fibers was too low to attempt a good correlation with the scattering data, thus only the total number of recorded fibers was used in the calibration procedure.

Least-square fits were made for each detector pair to determine which of the pairs would be most suitable for fiber identification work. Trial fits were first computed using all of the coincident and non-coincident regions, (as many as were permitted by either computer limitations or the number of samples). Regions of low significance were then eliminated, regions which showed similar coefficients were combined, and the subsequent fit was recomputed. This iterative process was continued until a satisfactory fit was achieved based on as few region combinations as necessary.

The  $\pm 45^\circ$  detector pair produced the best attainable least-square fit using only six variables. A plot of the fiber concentrations calculated using the least-squares fit versus the actual EM fiber data can be seen in Figure 12 for the Duluth samples. With a standard deviation of only .42 million fibers/liter, the quality of the fit is quite good, and suggests that the optical scattering method, once calibrated with sufficient EM data, is actually more accurate than the EM fiber analysis. When the number of pulse height-pulse ratio region combinations is reduced still further, the quality of the fit deteriorates somewhat. For instance, a four variable fit was obtained with a standard deviation of .61 million fibers/liter.

Of the 60 samples tested, only 10 percent were omitted, usually for obvious reasons such as excessive filter flocculent or fiber clumping. Seven of the 21 data points represent sample averages. A constant was added to the fitting equation to offset error which might shift the data. Electronic noise which could inadvertently be counted as an event is one such source of error. A random loss of fibers to container walls or in the EM analysis is also a possibility, as well as sample contamination.

Shown in Table 1 are the final region combinations and significance values used to produce the fit. The coefficient values correspond to the  $a'$ ,  $b'$ , and  $c'$ , etc. of equation (2) where the  $N_i$ s are the summed event rates of the listed region combinations. The significance values, defined as the absolute value of the product of the coefficient and the average event rate for each particular region combination yield a measure of the relative importance of each variable. As regions were selected to produce the best fit to the measured fiber concentrations, it became clear that only a few regions played an important role in particle identification and many of the peripheral regions supplied only small corrections to the fit. Thus the final selection of the peripheral regions was influenced by the statistical errors associated with the particular set of data used in the calibration.

TABLE 1. Coefficients for the  $\pm 45^\circ$  fit to Duluth filtered water.

#	COEFF.	SIG.	REGION COMBINATIONS
1	$-.136 \times 10^{-1}$	1.336	C-1, C-3, N-3, N-4, N-7
2	-.254	17.257	C-2, C-12, N-11
3	$.453 \times 10^{-1}$	3.937	C-7, C-10, N-2
4	$.595 \times 10^{-1}$	7.020	C-4, C-5, C-9, N-9, N-10
5	-.157	1.176	C-11
6	$.950 \times 10^{-1}$	11.819	C-6, C-8, N-8
C	.279		

The significance values and signs of the coefficients used for identification of particle types in filtration samples vary in comparison to the coefficients found for the samples of known particle types. For example, the coincident regions 6 and 8 associated with the most significant positive coefficient for filtration plant samples are also regions of high red clay ( $< 2 \mu\text{m}$ ) probability (see Figure 8), a background particle type which the fit for fibrous particles should suppress. The main types of background particulates in the Duluth filter effluent, however, are biological material, mostly diatom fragments and bacteria, and aluminum hydroxide globules from the filtering process. Thus it is not clear just how the test particle types such as red clay and tailings actually influence the selection regions for fibers in filtration samples, since the red clay and tailings may constitute an insignificant fraction of the background of non-fibrous material in the samples. Furthermore, the test samples for known particle types had different particle size distributions than those of the Duluth filtration plant samples. For example, about 25 percent of the amphibole fibers found in the amosite samples were greater than  $2 \mu\text{m}$  even though the samples were sized by centrifuge to less than  $2 \mu\text{m}$ . In contrast, most of the fibers in the Duluth water were less than  $1 \mu\text{m}$ .

Another factor which makes the interpretation of the coefficients difficult, has to do with the mathematical nature of the fitting equation. The condition necessary for a valid fit is not that one particle type be more probable than another in a given region, but more specifically, that changes in the probability differences (and ratios) exist from region to region.

One caution concerning the reliability of the fitting equation should be considered. If from sample to sample the concentration of a particular background particle type remains directly proportional to the fiber concentration, the coefficients will adjust to give a least-square fit to both types of particulates weighted toward the particle type which is more numerous. Then if the ratio of fibers to this background particulate should ever change, the equation would predict incorrect fiber levels. In view of the fluctuating levels of the various suspended solids found at the filter plant intake, it is unlikely that this will be a problem provided enough samples are taken over a long enough period to allow for sufficient variability.

A plot of the total number of events during each 10 minute test period versus the EM fiber concentrations for a series of filtration samples is shown in Figure 13. Each point in Figure 13 was averaged identically to the manner used in establishing the original calibration for fiber counts in filtration samples. The large dispersion of the points in Figure 13 indicates, as suspected, that the ratio of fibers to the total number of suspended particles is not constant, supporting the fact that the calibration actually represents the fiber count. This result also suggests that a straightforward particle count alone would be of limited usefulness for detecting the actual fiber concentrations. An electron microscope estimate on all particulate constituents of filtration plant samples would be helpful in interpretation of the pulse height-pulse ratio categories found for the filtered water samples.

Least-square fits to the EM "total" fiber concentrations are shown in Figures 14 - 16 for each of the other three detector pairs. The respective coefficients for equation (2) are found in Tables 2 - 4. For the  $\pm 90^\circ$  and

TABLE 2. Coefficients for  $\pm 90^\circ$  fit.

#	COEFF.	SIG.	REGION COMBINATIONS
1	$.763 \times 10^{-1}$	2.77	C-11, N-2, N-3, N-5, N-12
2	.144	12.59	C-1, C-2, C-5, C-7, C-8, C-10
3	.162	13.17	C-4, C-6, C-12, N-7
4	$.242 \times 10^{-1}$	.69	N-9
C	-.714		

TABLE 3. Coefficients for the  $+45^{\circ}, -135^{\circ}$  fit.

#	COEFF.	SIG.	REGION COMBINATIONS
1	$.267 \times 10^{-1}$	3.45	C-3, 1-4, 2-2, 2-5, 2-9, 2-12
2	$-.545 \times 10^{-1}$	1.35	C-8, 1-10, 2-6
3	-.237	9.94	C-5, C-6, C-7, C-12
4	.343	14.12	C-9, 2-8, 2-11
5	.134	2.56	C-10, 1-2
6	-.290	5.98	1-1
C	.415		

TABLE 4. Coefficients for the  $+45^{\circ}, +135^{\circ}$  fit.

#	COEFF.	SIG.	REGION COMBINATIONS
1	$.843 \times 10^{-1}$	.77	C-5
2	$-.679 \times 10^{-1}$	1.66	C-8
3	$-.500 \times 10^{-1}$	3.47	1-3, 1-5, 1-8, 1-12
4	$.939 \times 10^{-1}$	1.56	1-9, 1-10
5	$.612 \times 10^{-1}$	7.91	1-1, 1-4, 1-6, 2-5, 2-6, 2-8 2-11
6	-.352	2.73	2-1
C	.996		

+ 45° with - 135° fits, the EM data and sample averaging were identical to that used for the ± 45° case. However, a smaller amount of data was available for the + 45° and + 135° detector pair. The ± 90° fit was obtained with only four variables since little improvement was found by using more. This together with the point dispersion of Figure 14 indicates poor resolution of the ± 90° detector pair. Six variables were needed to produce reasonably good fits for the other two detector pairs.

The standard deviation of these cases is about double that of the ± 45° case, reflecting the fact that the repeatability was the best for the ± 45° detector pair. The increased zero stability due to the lower gain settings is the main difference between the ± 45° case and the other three detector pairs. Both zero drift and the ± 1 bit accuracy of the A/D converter can substantially influence the number of small peaks which exceed the cutoff level. Another source of error which has also been mentioned earlier is due to the statistical fluctuations in the number of fibers measured using EM techniques. Even after averaging the samples, each data point usually represented fewer than 50 fibers. Assuming that the EM data fluctuations are random and can be described by the usual Poisson statistics, a best-care error of about ± 15% is implied. A similar source of error results from the statistical uncertainty associated with the number of counts in each pulse-height region combination. Although for a typical sample as many as 1000 events may have been detected, once these are split into their respective regions and inserted into the fitting equation, the possible error can become appreciable.

The EM data for the Seattle samples consisted of counts of amphibole and chrysotile fibers with no quantitative information on the other background particulates. Because the number of samples which contained significant amount of both types of fibers were low, the two fiber counts were summed to yield total fiber concentrations. The ± 45° detector pair again produced the best results. The Seattle samples included both raw and finished water with greatly differing fiber concentrations and background material. Separate comparisons of EM and predicted concentrations from optical data are shown in Figures 17 and 18 for the raw and filtered samples respectively. Six variables were used for each calibration fit with the coefficients found in Tables 5 and 6.

The finished water samples, Figure 18, yield a greater dispersion of the points. This can be easily accounted for by the statistical uncertainty associated with the EM data. Due to an insufficient number of samples, averaging was not practical, and some of the points represent as few as 5 to 10 fibers. Furthermore, especially for the finished water, a fair percentage of the fibers were often less than .5 µm in length and it is not known whether such small fibers would produce scattering peaks which would exceed the cutoff level. It should also be mentioned that the average sample fiber concentration was quite low compared with that of the raw water, or even the previously discussed Duluth samples. Thus, only a small percentage of the scattering events were produced by fibers.

TABLE 5. Coefficients for the fit to Seattle raw water.

#	COEFF.	SIG.	REGION COMBINATIONS
1	$.882 \times 10^{-1}$	55.49	C-2, N-1
2	$.213 \times 10^{-1}$	18.63	C-4, C-10, N-5
3	.112	155.73	C-6, N-8
4	.153	76.23	C-12
5	-.201	114.18	C-8
6	$-.526 \times 10^{-1}$	72.27	N-4, N-6
C	$.430 \times 10^{-1}$		

TABLE 6. Coefficients for the fit to Seattle filtered water.

#	COEFF.	SIG.	REGION COMBINATIONS
1	$-.263 \times 10^3$	.05	C-1, N-3, N-7, N-10
2	$-.825 \times 10^{-3}$	.06	C-5, N-5, N-12
3	$.618 \times 10^{-4}$	.01	C-3, C-10
4	$.143 \times 10^{-2}$	.42	C-2, N-1, N-4, N-6, N-8
5	$-.572 \times 10^{-2}$	.41	N-9
6	$.646 \times 10^{-3}$	.19	C-6, C-8, C-12, N-2
C	$.374 \times 10^{-1}$		

The raw water samples, for which as many as 200 fibers were counted, produced a much better fit, Figure 17. To ensure that no more than one particle was usually in the beam, many of the raw samples were diluted prior to testing.

## SECTION 8

### REFINEMENTS TO THE APPARATUS

In the past six months much time has been spent incorporating a microcomputer (Processor Technology, Sol-20) into the scattering equipment. A number of distinct advantages are realized. The microcomputer has its own seven-channel analog to digital converter with twice the resolution as the one previously used. The increased accuracy plays special importance in the determination of the baselines and in the measurement of small peak heights where small errors can influence the number of events which exceed the cutoff level. In addition, the microcomputer allows us to sample any number of the six detectors at any desired rate up to about 200 Hz, which reduces the uncertainty in the peak-height measurements inherent in the previous slow 15 Hz rate. Operator interaction is also greatly reduced by the microcomputer. In the past it was necessary to secure the large university computer by phone and continually reopen the data file every two minutes as the test progressed. Thus test durations of over 10 to 20 minutes were impractical. Using the microprocessor, the only limitation is due to an overflow of the microcomputer memory which for low concentration samples can accommodate runs of many hours. Finally, and perhaps the most important feature, the microcomputer will eventually make the apparatus portable, and more useful as a research tool or an on-line monitoring device.

After interfacing the microcomputer to the detectors, a machine language program was written and debugged to do the following: 1) simultaneously sample three detectors at 60 Hz rate, 2) find the baseline (zero) of each detector, 3) search for peaks at each detector and determine if they are coincident with peaks found at the other two detectors, and 4) store the peak heights and coincidence information in the microcomputer memory. The program divided the events into seven categories: three non-coincident, one for each detector, and four coincident, one for each of the three combinations of two detectors, and one indicating complete overall coincidence. Since the complexity of the program and data analysis increases rapidly with the number of detectors that are included, the program was written to handle only three detectors simultaneously.

The sampling rate of 60 Hz, which is conveniently derived from the power line, was chosen so that the A/D converter would sample in phase with the 60 Hz noise present on the detector outputs, thus further reducing sampling errors. The cutoff level has also been lowered somewhat to improve the small peak-height sensitivity. After the microcomputer memory is full or the desired test duration is reached, the peak-height information is sent by phone to the university computer. Although this greatly facilitates the



research, the use of another computer will be unnecessary in the fiber detection system once a satisfactory calibration of the instrument with the EM data is achieved.

Samples were tested at two different combinations of three detectors: 1)  $\pm 45^\circ$  with  $+ 135^\circ$  and 2)  $\pm 135^\circ$  with  $+ 45^\circ$ . So far the data has only been analyzed for the first of these cases, chosen because of the promise shown earlier by the  $\pm 45^\circ$  fits and by the pronounced signatures seen at the  $+ 135^\circ$  detector for the known particle types. Programs have been written to further subdivide each coincidence type into three categories according to peak-heights in the  $+ 135^\circ$  detector. A frequency distribution plot of the  $- 45^\circ$  versus the  $+ 45^\circ$  pulse heights was then made for each group.

When a new series of Duluth samples with EM data became available, including both raw and finished water, the samples were tested using the new three-detector method. Many of the samples were tested repeatedly, usually at least a few days later, as a check on reliability. The results confirm a phenomenon first pointed out by Tom Biele at the Duluth Filter Plant - the number of particles in the finished water samples increases with time. For a few of the pilot plant effluent samples, for instance, the total number of events for a given test duration increased by nearly a factor of ten over a two week interval. The continuing precipitation of the aluminum hydroxide which is added in the filtration process is believed to be responsible. The effect was not considered in the original testing of Duluth samples because they were scanned optically a number of days after their filtration date at which time the samples had stabilized.

Before applying the fitting programs to the new data, the frequency distributions, three for each of the seven categories of coincidence events, were subdivided into a total of 84 regions in a manner which accented the differences observed for the known particle types samples. Next, a program was written which, after finding the number of events per region for each sample, computed the relative independence of the 84 regions. Finally, the number of regions was reduced to a total of 24 by combining regions which displayed little independence.

Shown in Figure 19 is a least-square fit to the total fiber concentrations of the finished water samples. The term "total fibers" refers to the previous discussion concerning the Duluth EM data. Six variables consisting of various combinations of the 24 regions were used. Since the average number of EM observed fibers per sample was around two to three times higher than that of the previous Duluth water, the samples were not combined and averaged. About 30% of the sample points, however, do represent less than 20 fibers, which may account for much of the point dispersion. Thirty minute optical scans were usually employed.

A seven variable fit for determination of amphibole fibers concentration is shown in Figure 20. The quality of the fit is as good as one can expect considering the small number of observed fibers. In fact, 16 of the 23 points represent less than 6 fibers per sample.

Since it was not possible to test each sample immediately after it was drawn, many of the samples still contained an abundance of aluminum hydroxide particles at the time they were tested. The fact that a satisfactory fit was obtained suggests that the scattering method is able to distinguish fibers among a large amount of the precipitate.

For comparison, plots of both the amphibole and total fiber concentrations versus total particle concentrations are shown in Figures 21 and 22 for the two respective sets of data. The total particle counts were obtained by the personnel at the Duluth Filter Plant using a Hiac, Model PC 320, particle counter with a minimum particle-size detection limit of 1.0  $\mu\text{m}$  (average particle dimension). The plots point out the great uncertainty encountered by using a single-detector particle counter for fiber level measurements. For example, in Figure 22 two of the points (represented by triangles) which were plotted at nearly the same fiber concentrations differed in their total particle count by over a factor of 100. In contrast, the fiber concentrations of these same two samples were predicted accurately using the three-detector scattering fit.

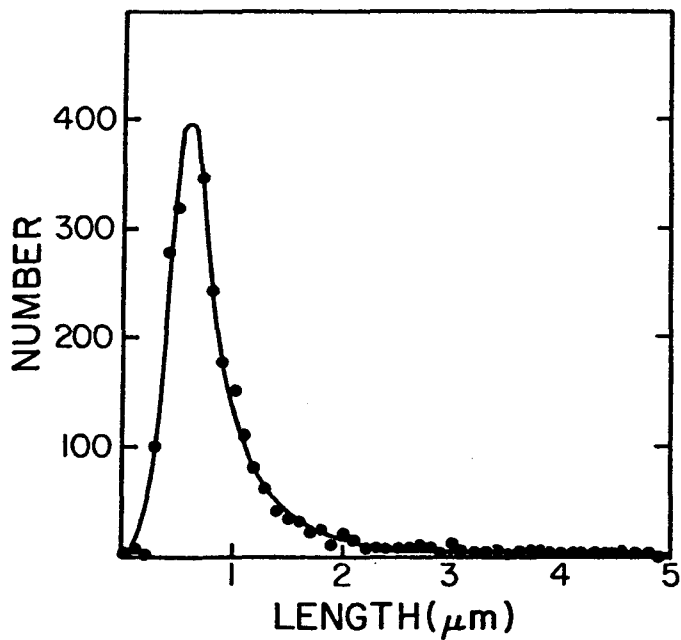
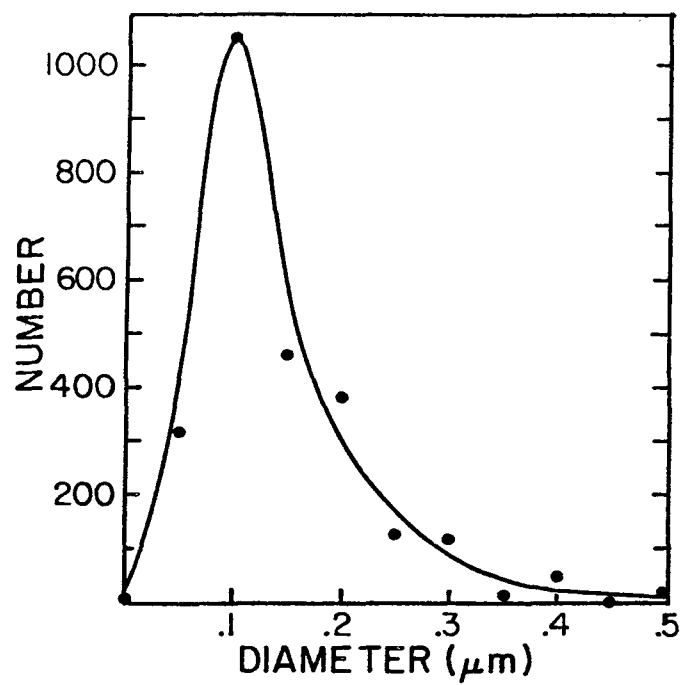


Figure 1. Size distribution of fibers found in Duluth drinking water. (Taken from electron microscope data on 50 samples drawn in 1977.)

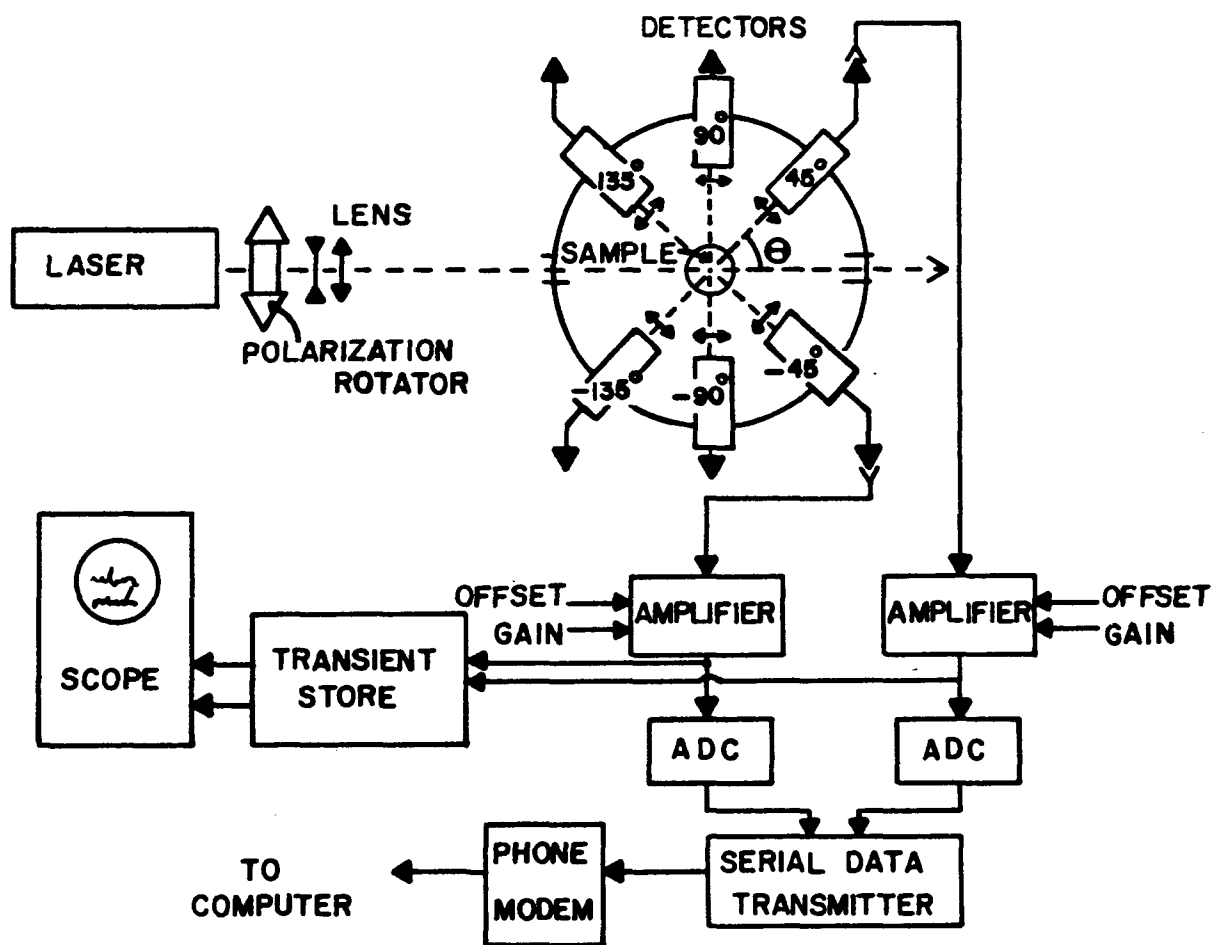


Figure 2. Block diagram of apparatus.

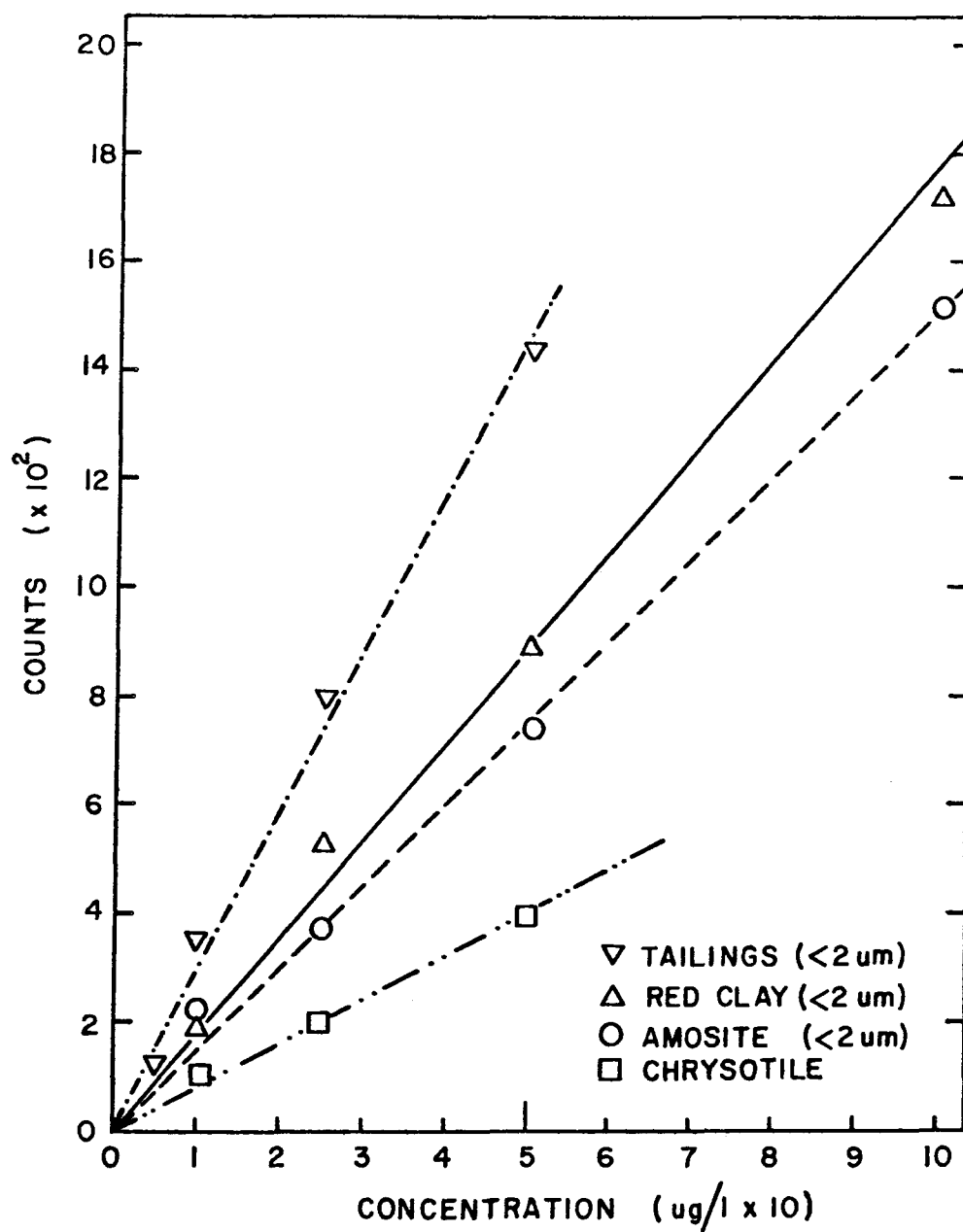


Figure 3. Number of events at the  $\pm 45^\circ$  detector pair versus concentration for each particle type.

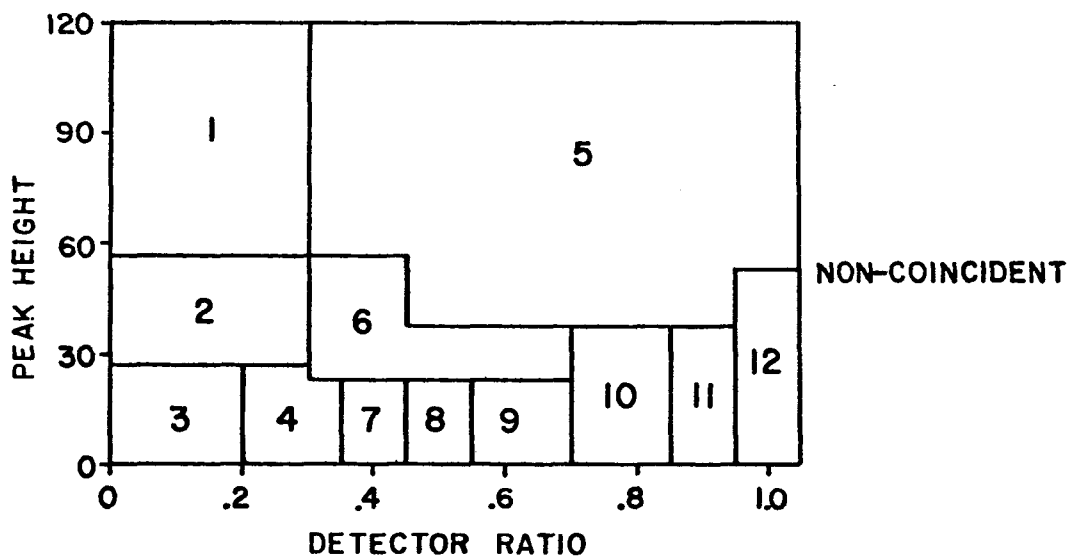
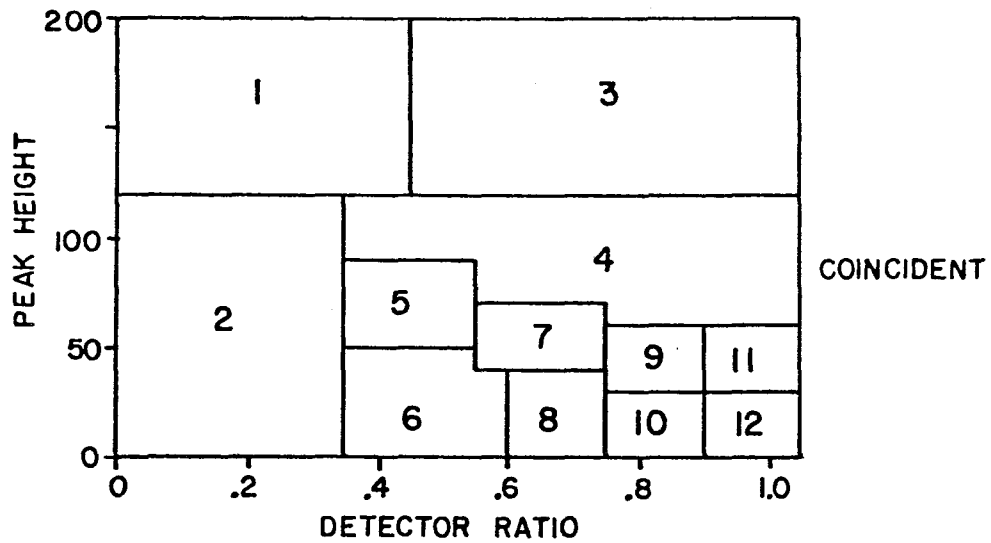


Figure 4. Region assignments for the  $\pm 45^\circ$  detectors.

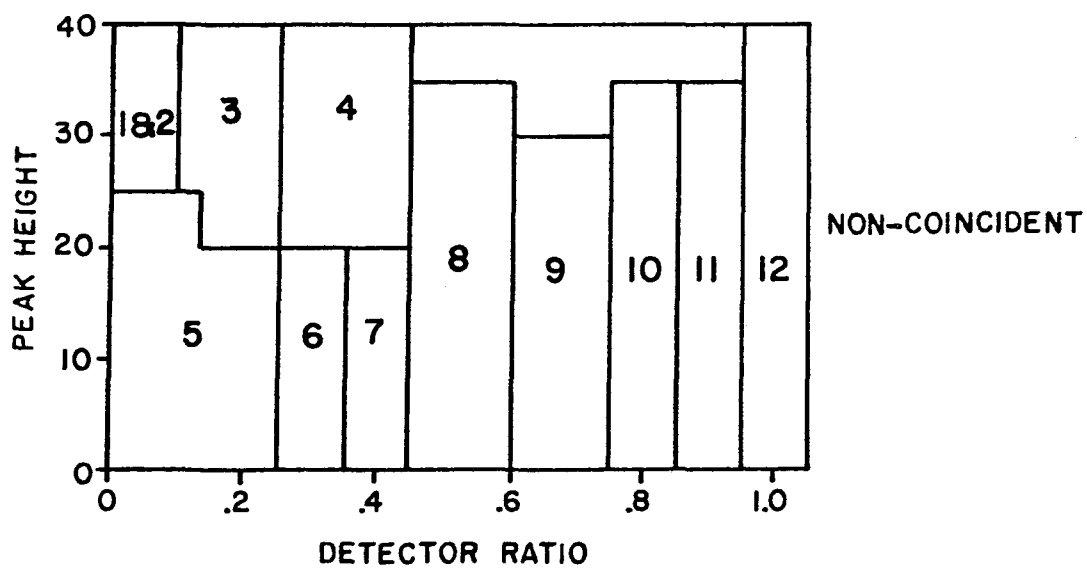
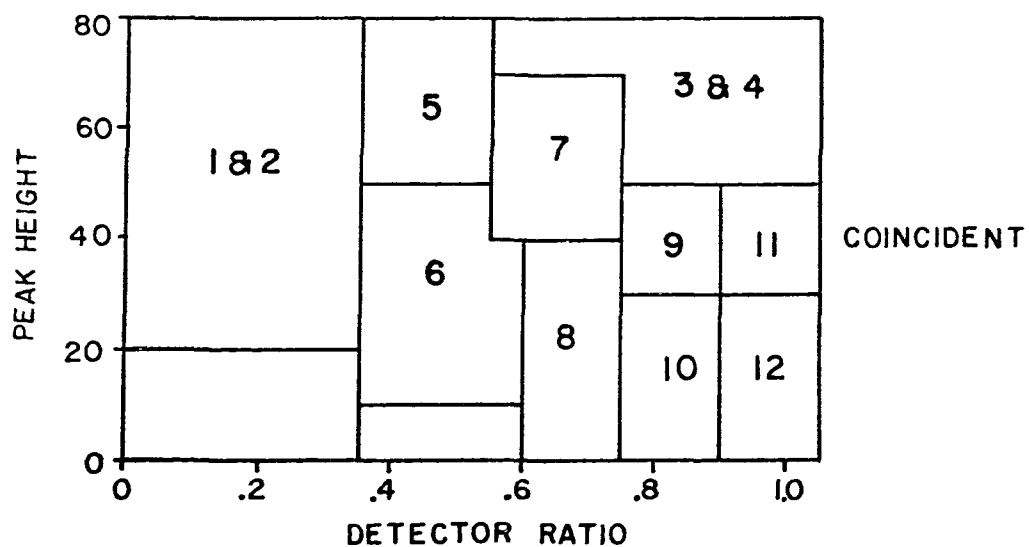


Figure 5. Region assignments for the  $\pm 90^\circ$  detectors.

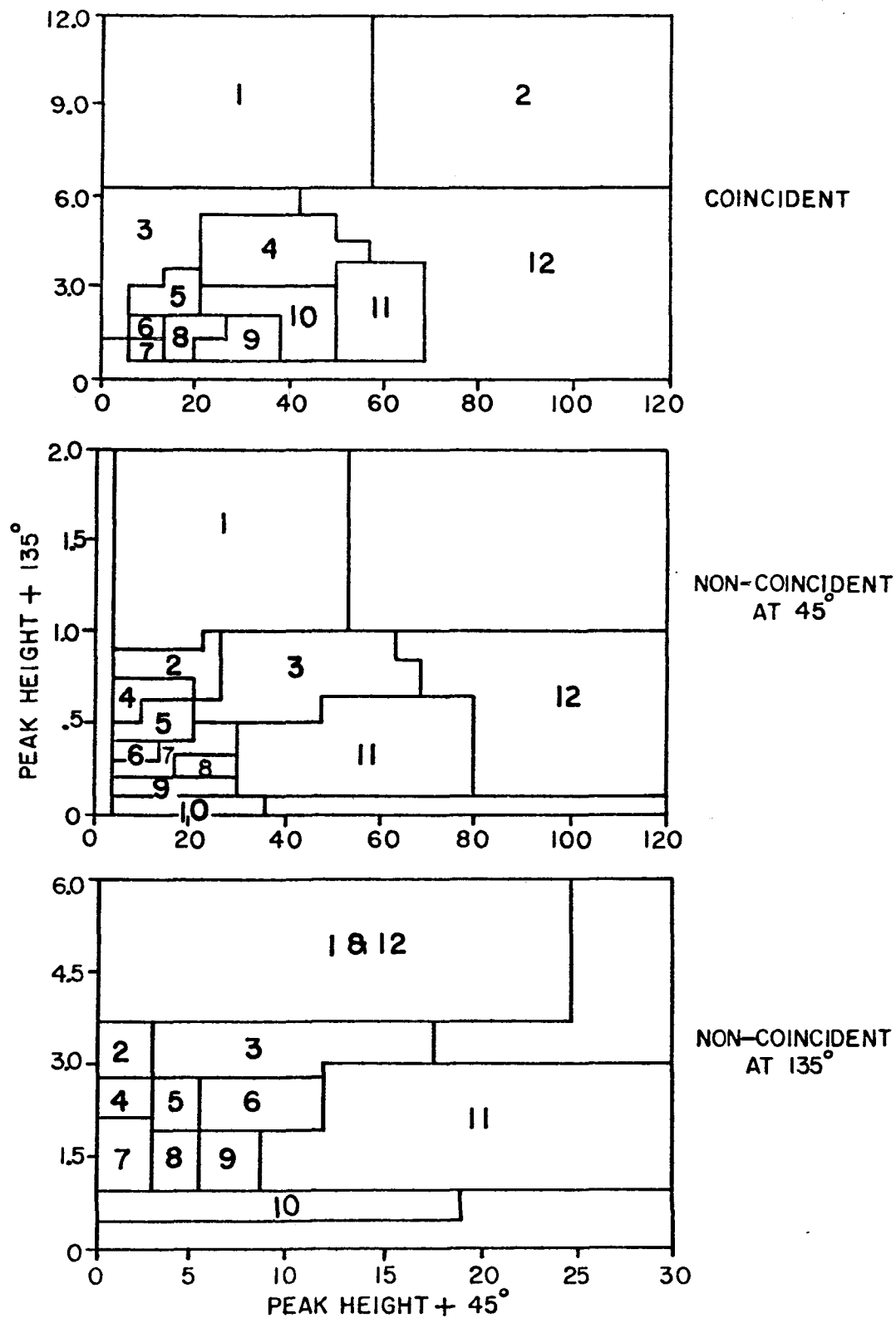


Figure 6. Region assignments for the + 45° and + 135° detectors.



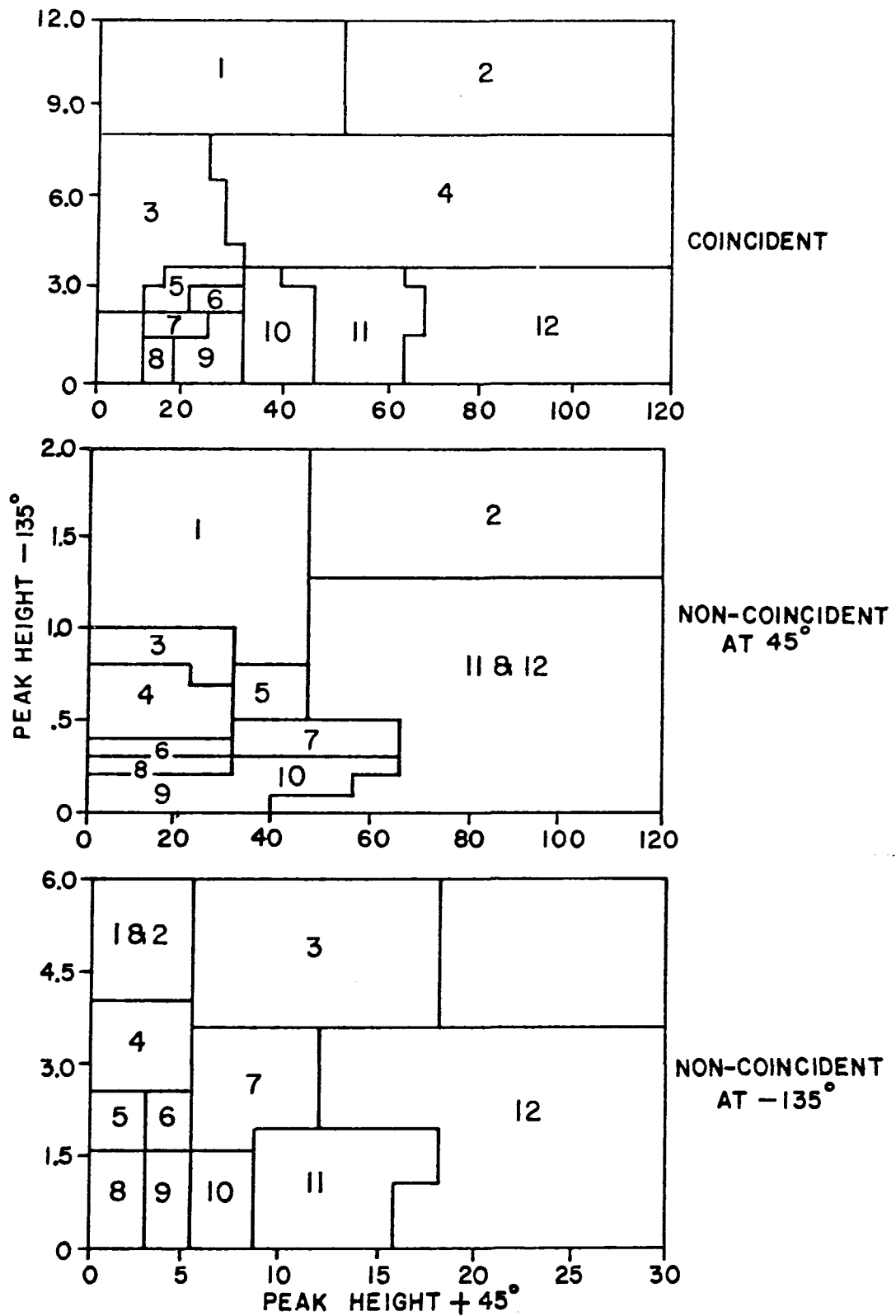


Figure 7. Region assignments for the + 45° and - 135° detectors.

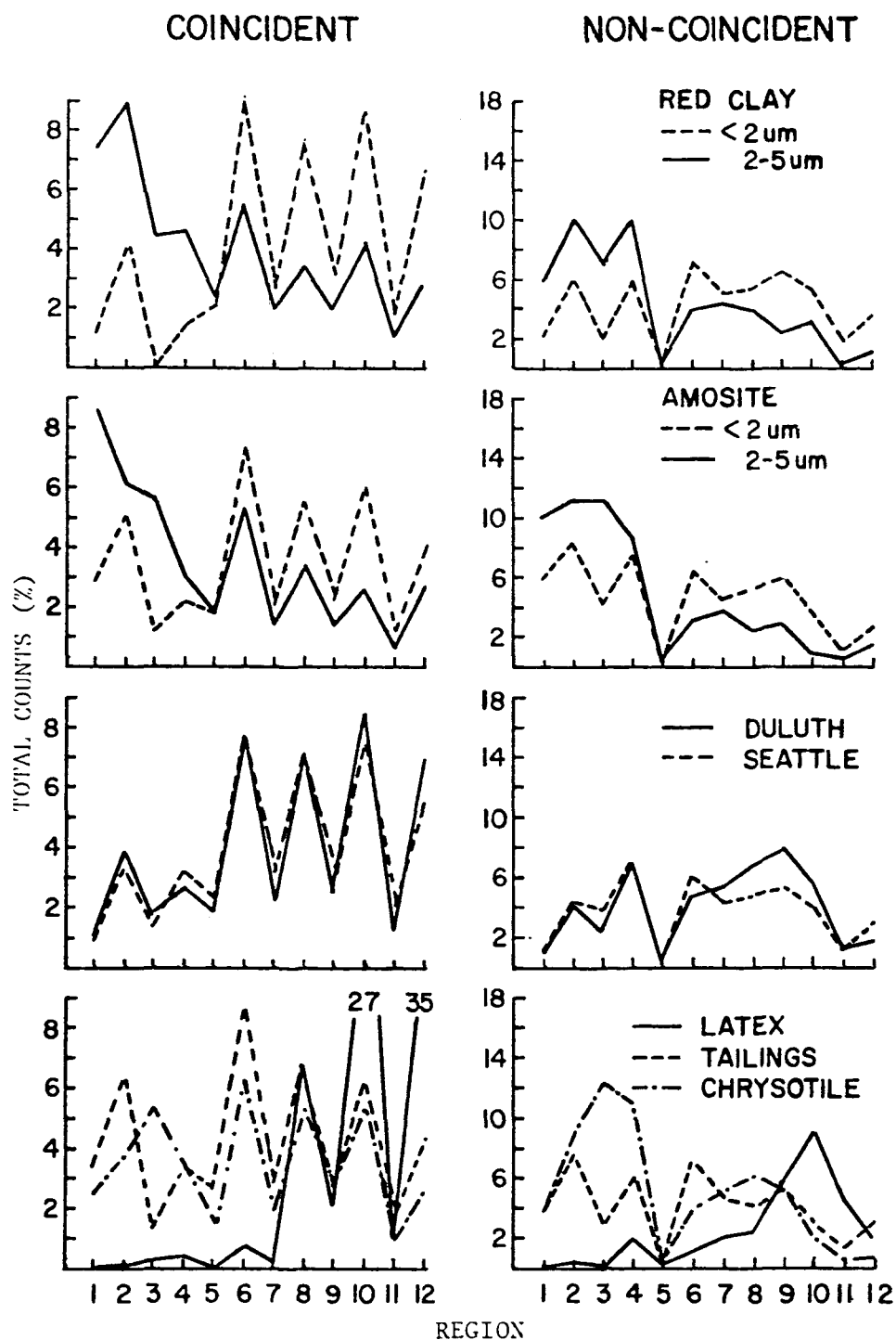


Figure 8. Percent of total counts versus counting region at  $45^\circ$  for each particle type.

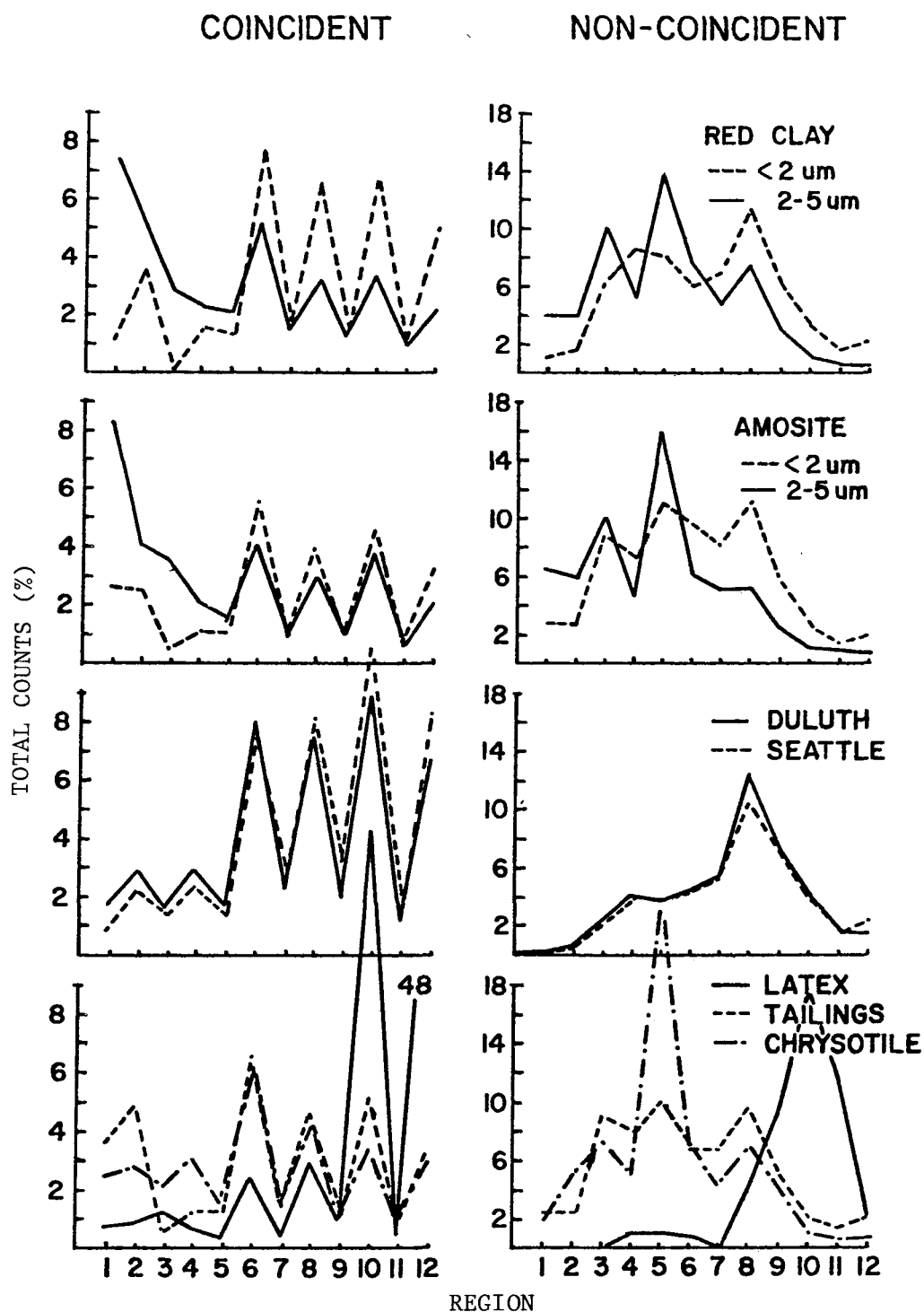


Figure 9. Percent of total counts versus counting region at  $\pm 90^\circ$  for each particle type.

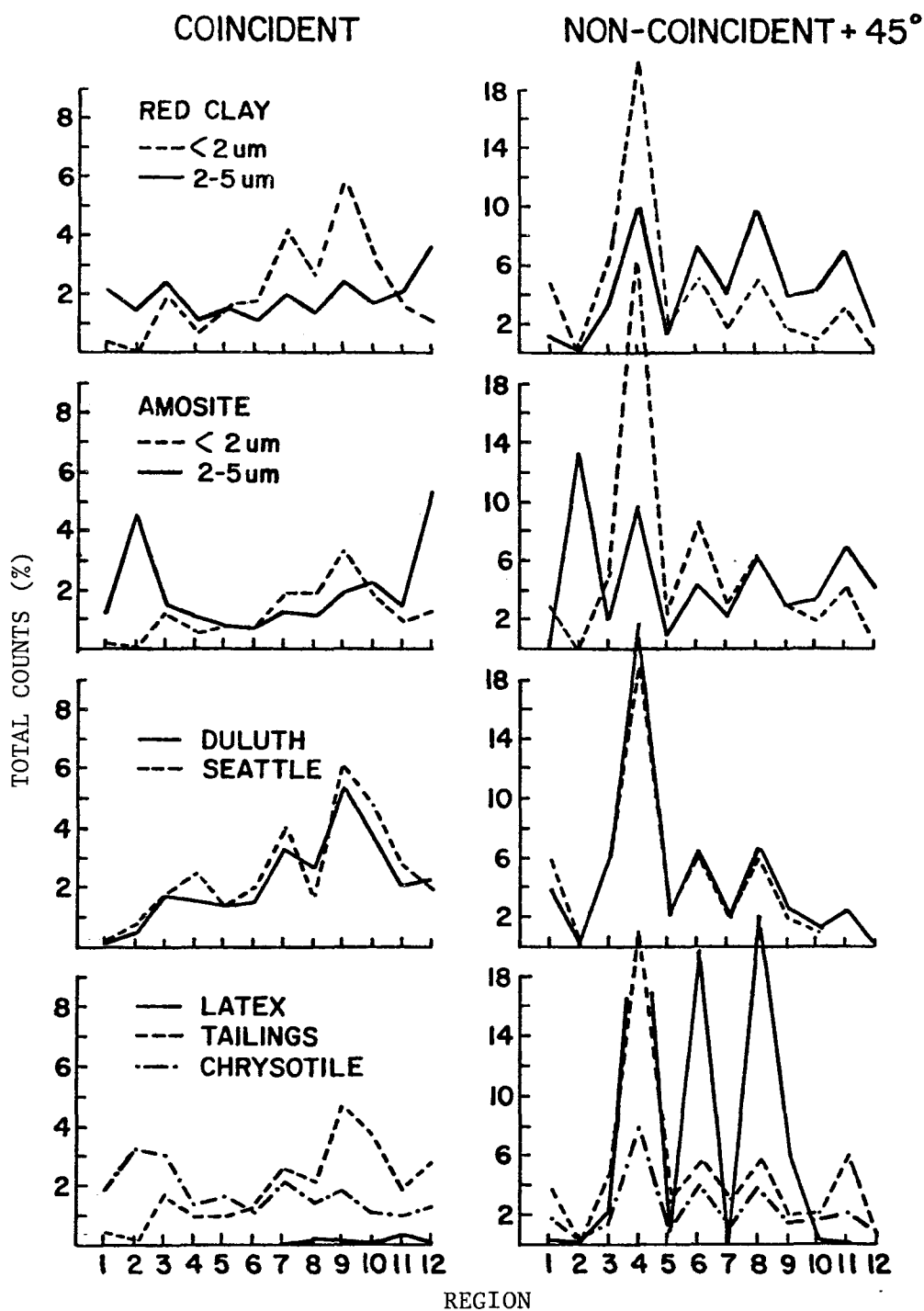


Figure 10. Percent of total counts versus counting region at + 45°, - 135° for each particle type. (continued on following page)

# NON-COINCIDENT AT -135°

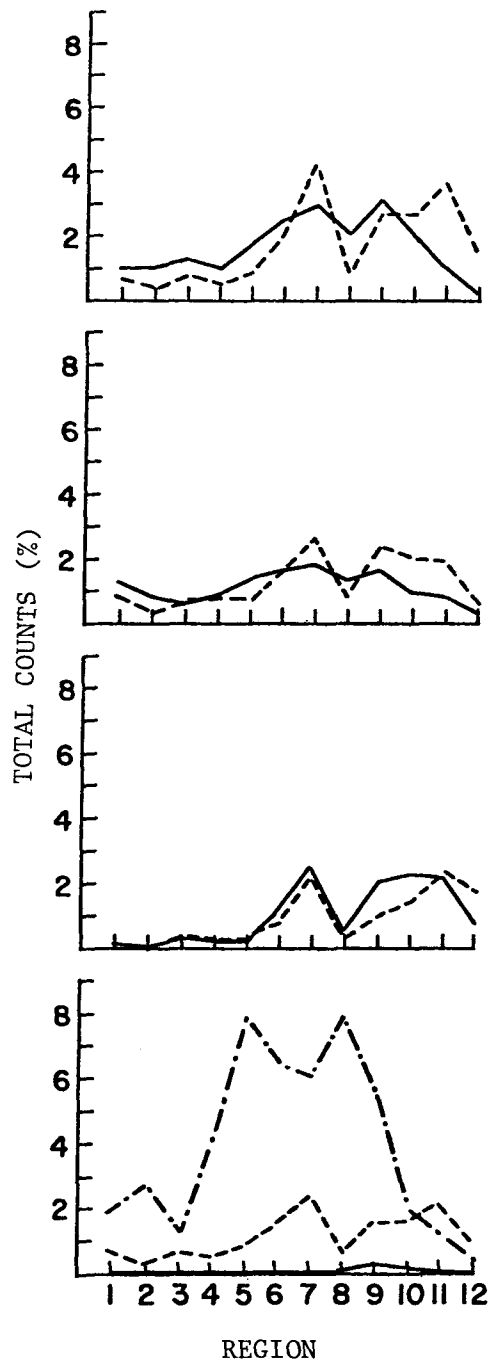


Figure 10 continued.

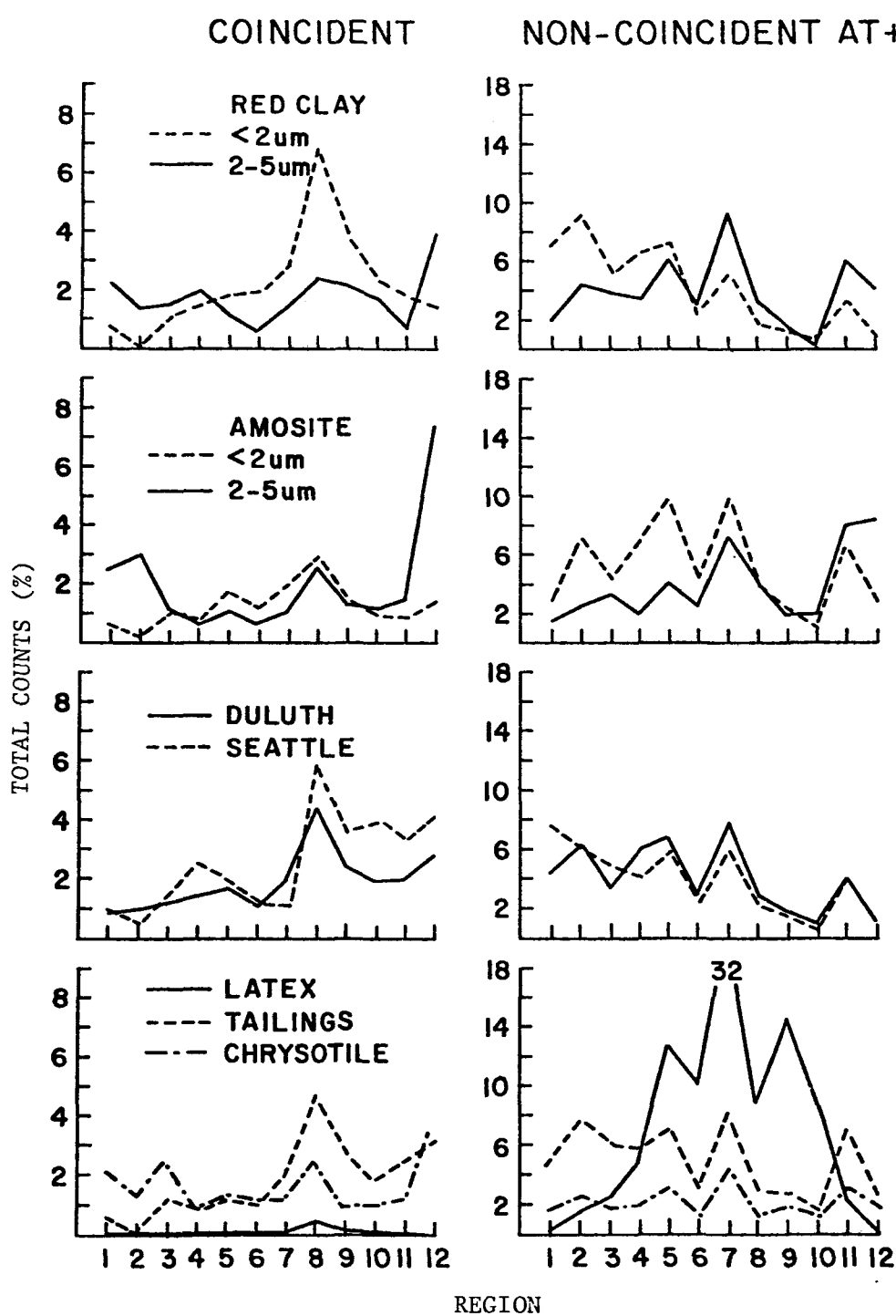


Figure 11. Percent of total counts versus counting region at + 45°, + 135° for each particle type. (continued on following page)

# NON-COINCIDENT AT +135°

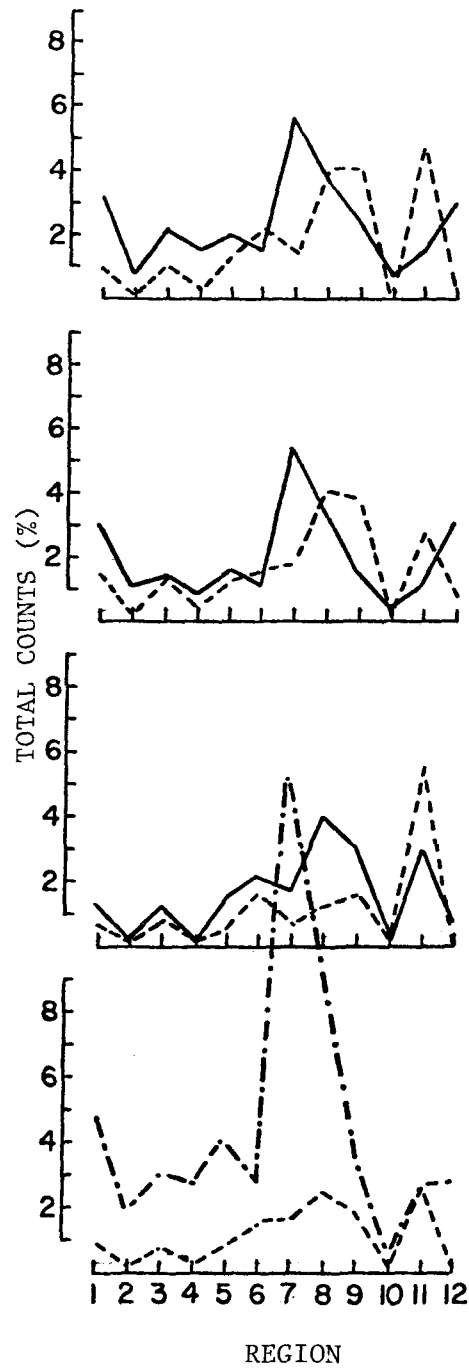


Figure 11 continued.

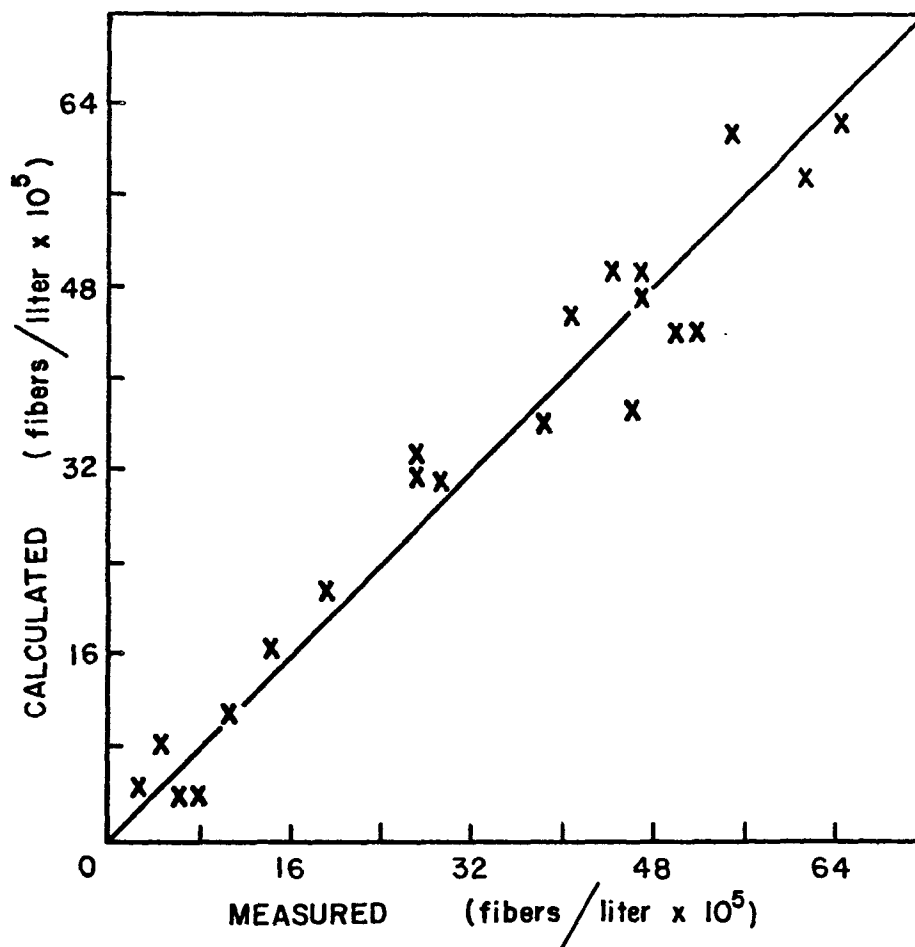


Figure 12. Predicted versus measured total fibers for Duluth water samples and  $\pm 45^\circ$  scattering angles.



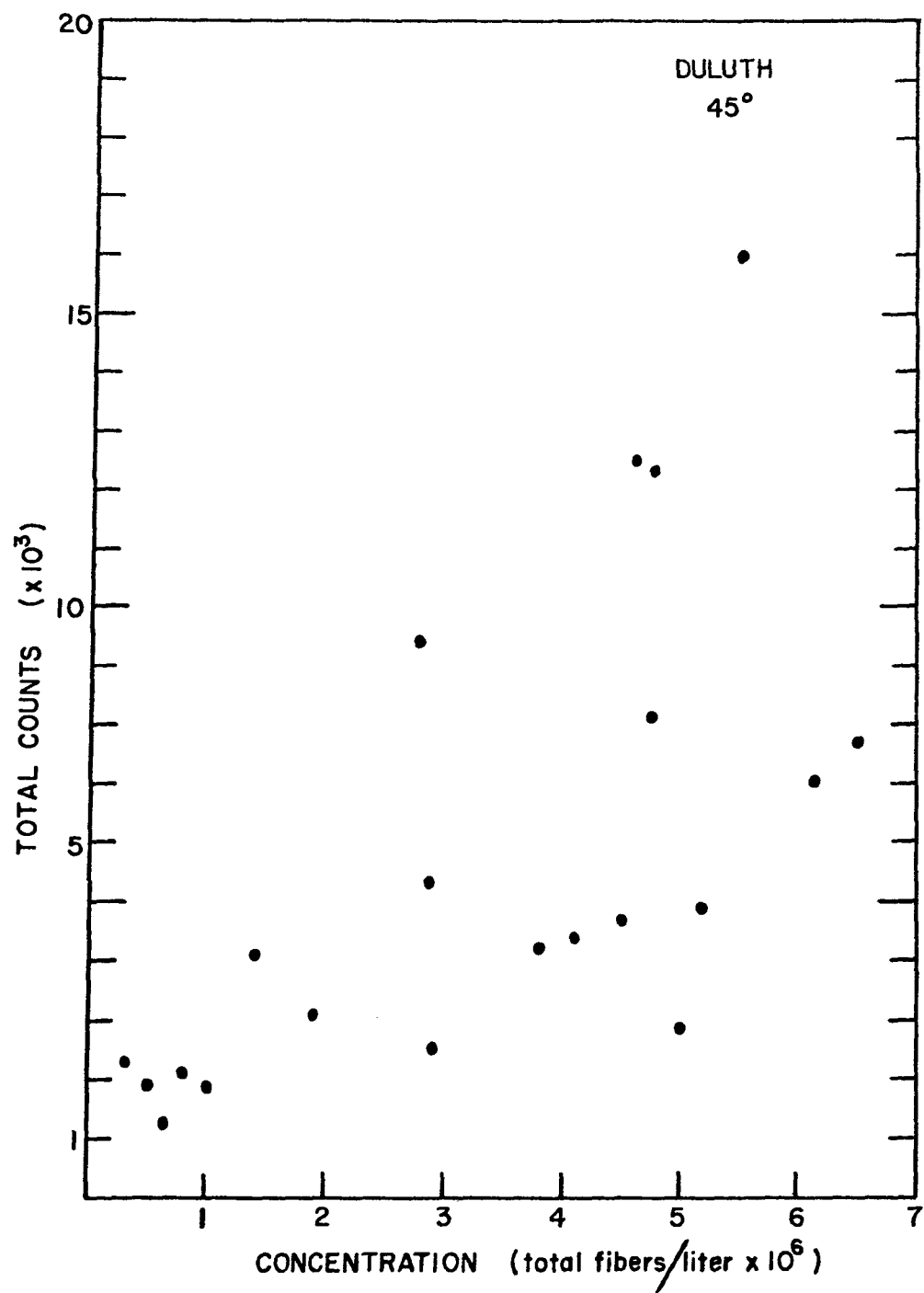


Figure 13. Total counts at  $\pm 45^\circ$  versus EM total fiber concentrations.

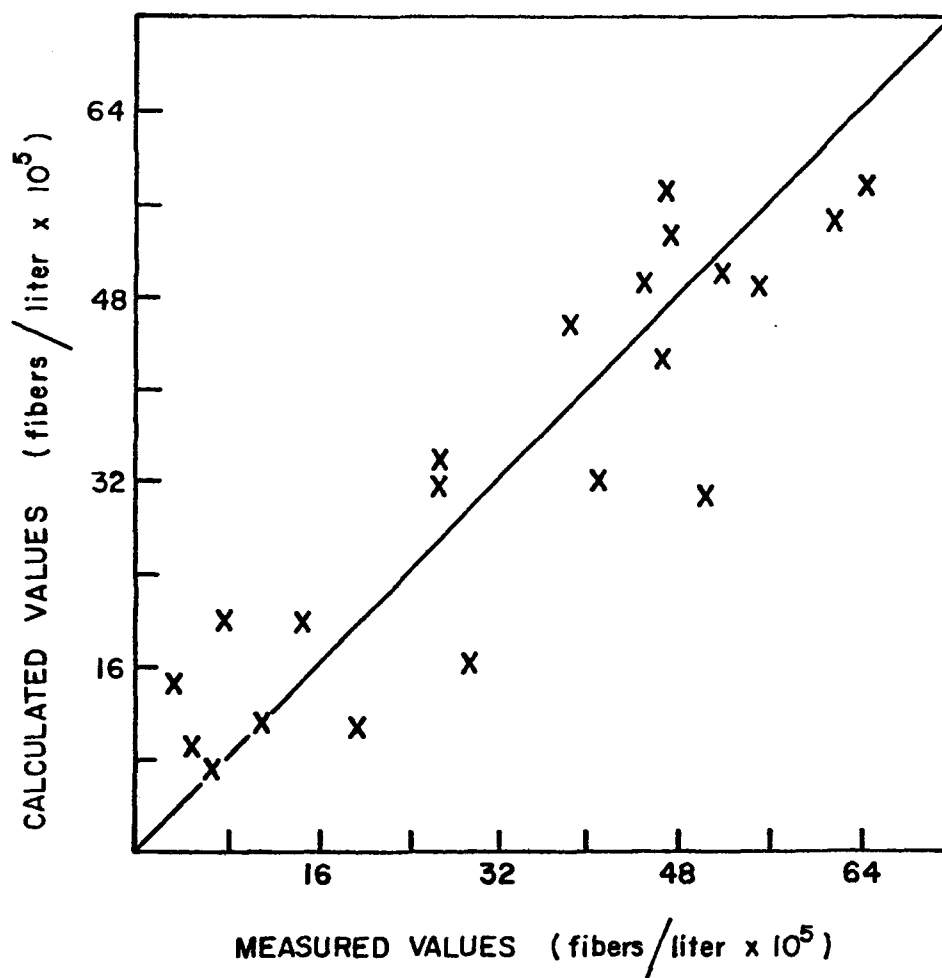


Figure 14. Predicted versus measured total fibers for Duluth water and  $\pm 90^\circ$  scattering angles.

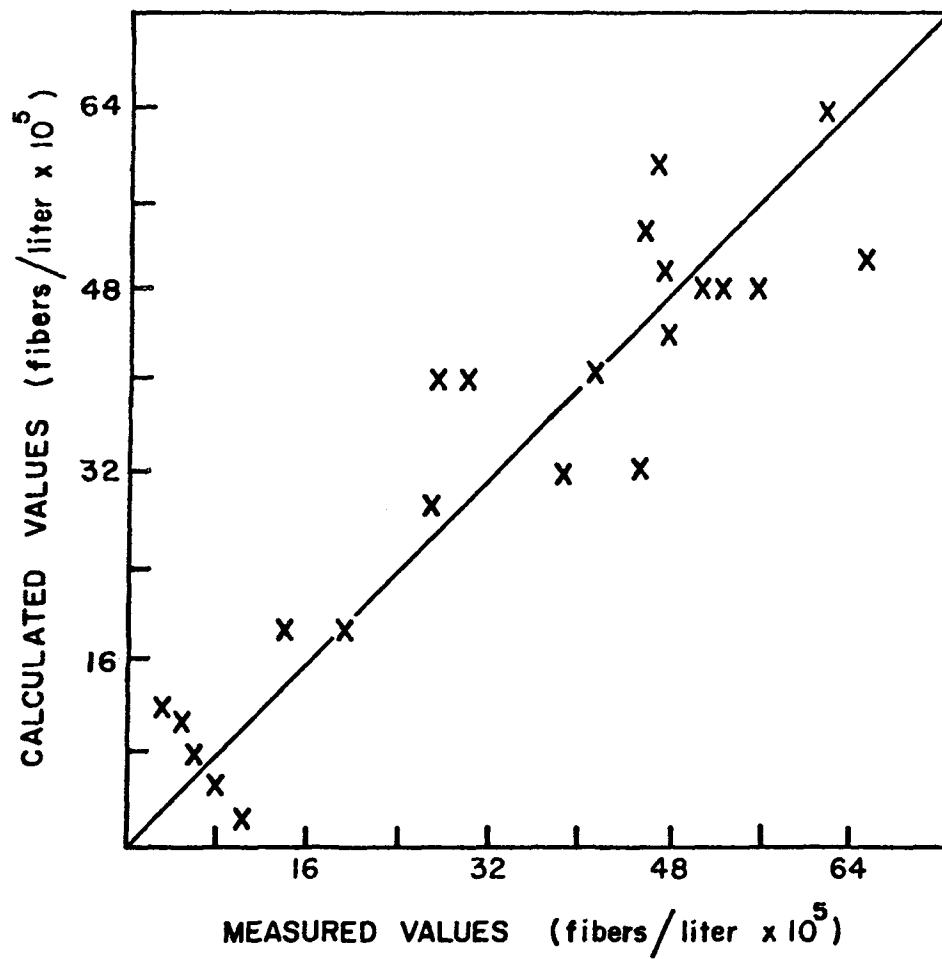


Figure 15. Predicted versus measured total fibers for Duluth water and + 45°, - 135° scattering angles.

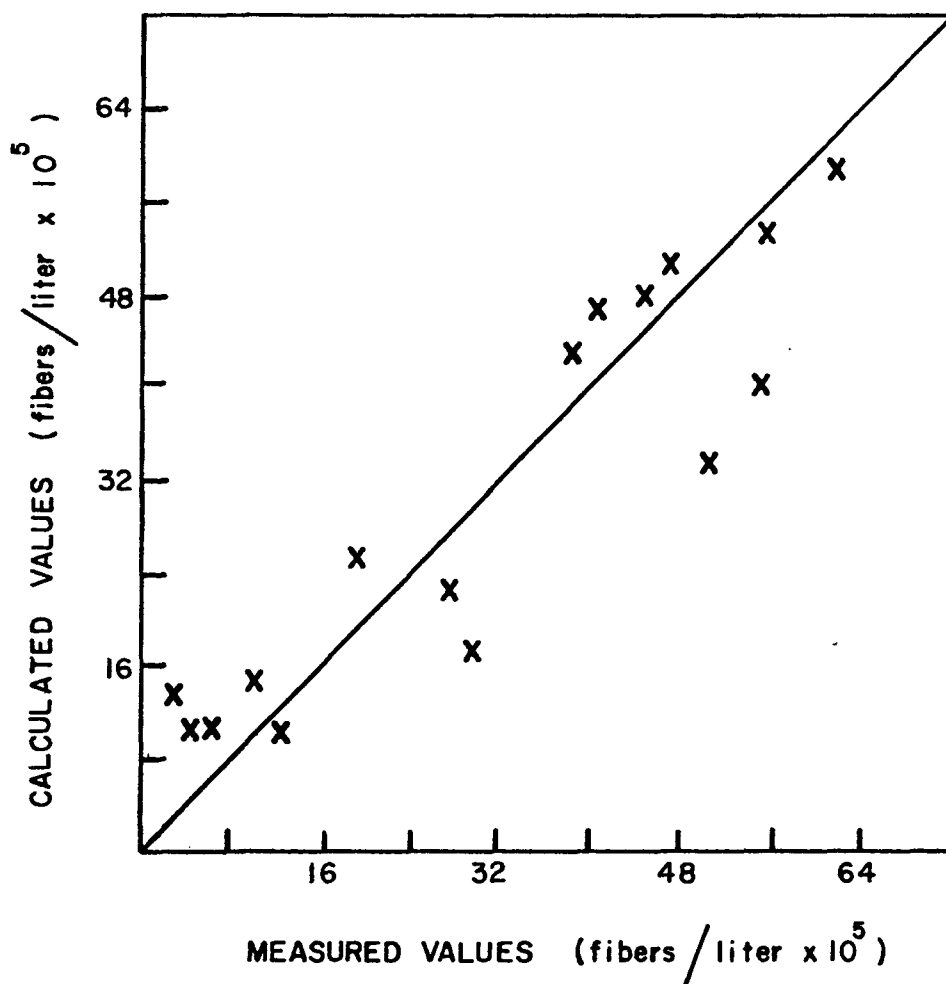


Figure 16. Predicted versus measured total fibers for Duluth water and + 45°, + 135° scattering angles.

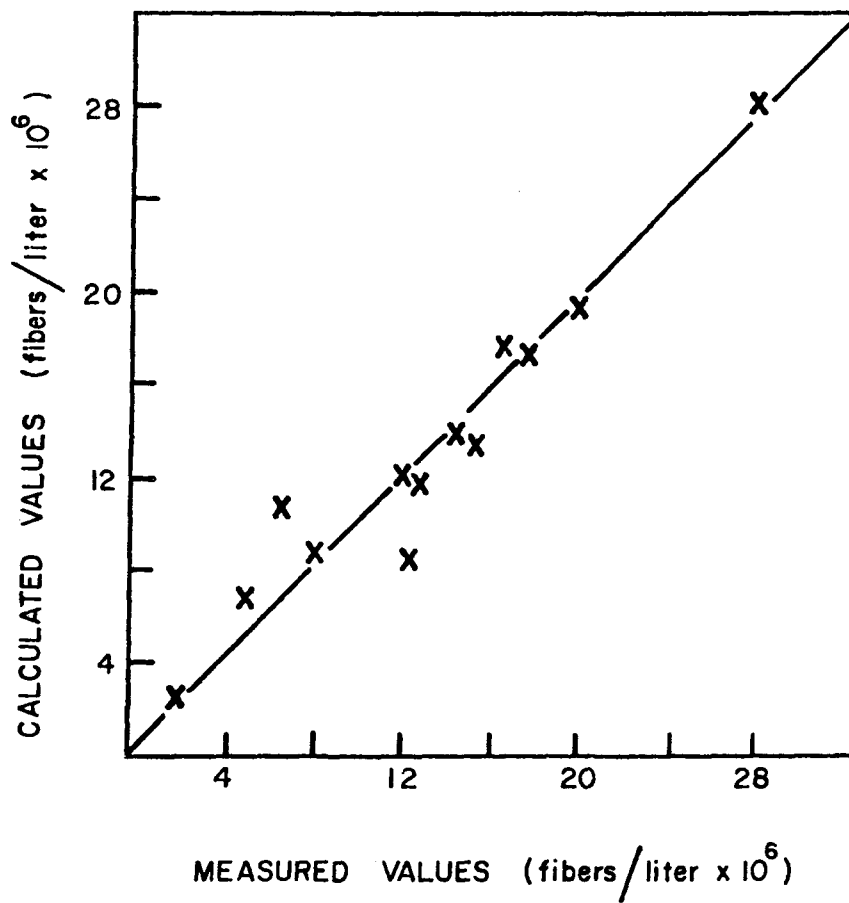


Figure 17. Predicted versus measured total fibers for Seattle raw water.

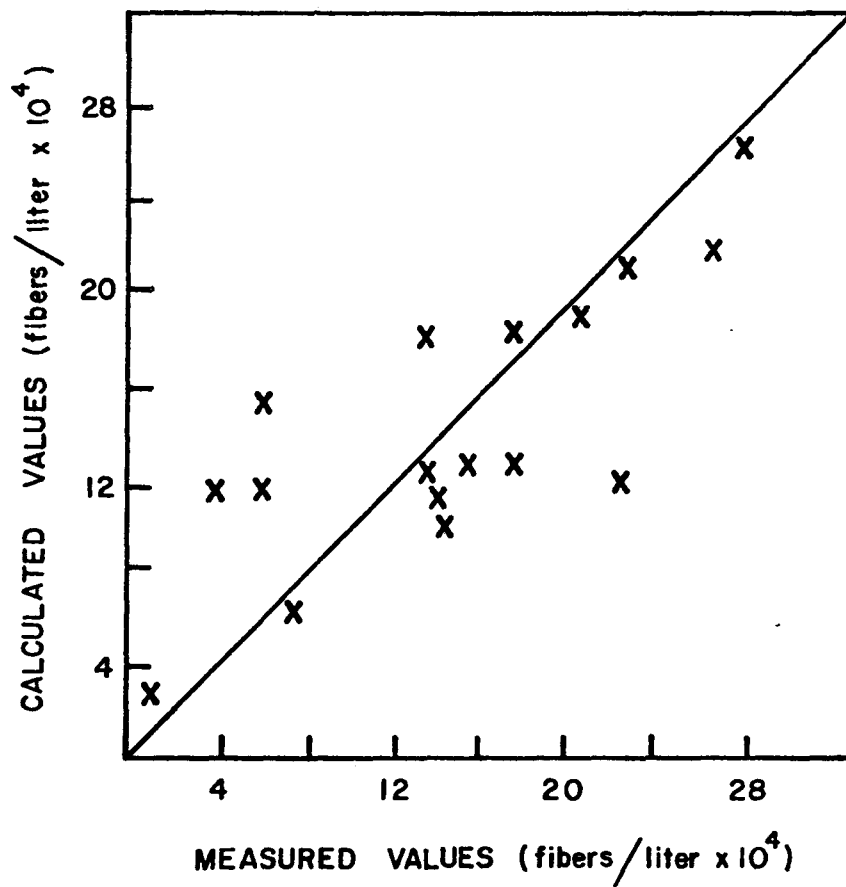


Figure 18. Predicted versus measured total fibers for Seattle finished water.

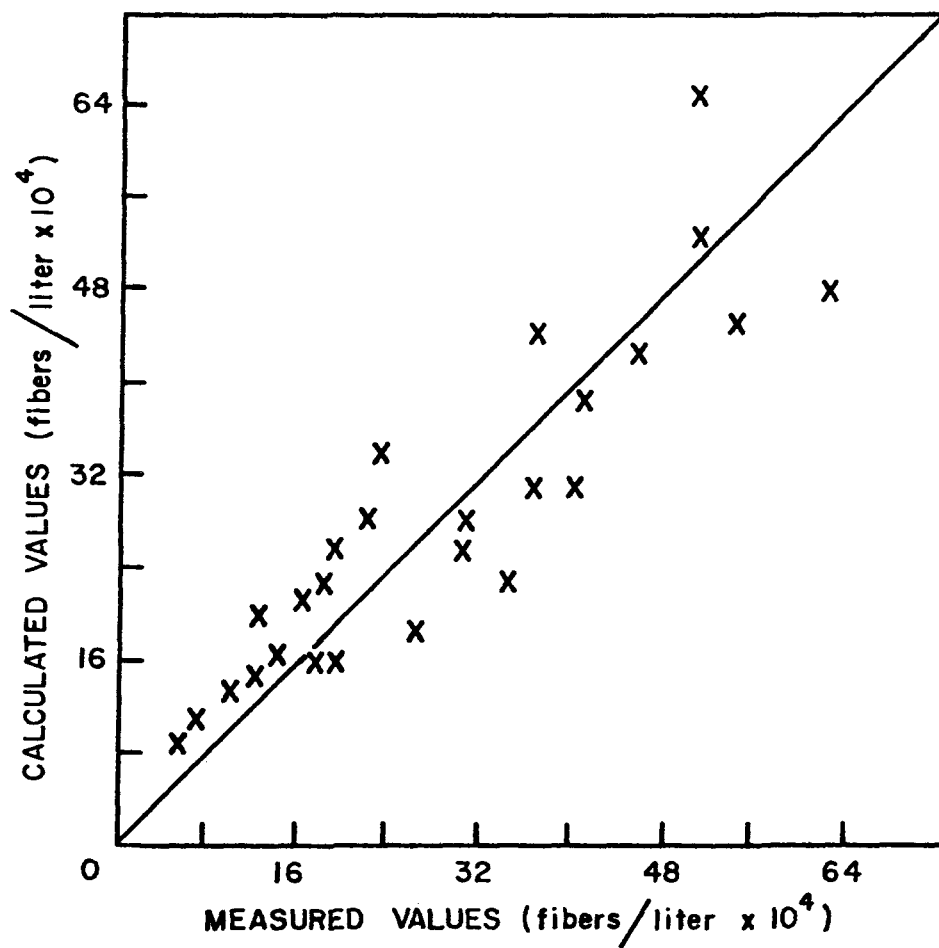


Figure 19. Comparison of predicted total fibers and EM measurements for data collected using the modified apparatus.

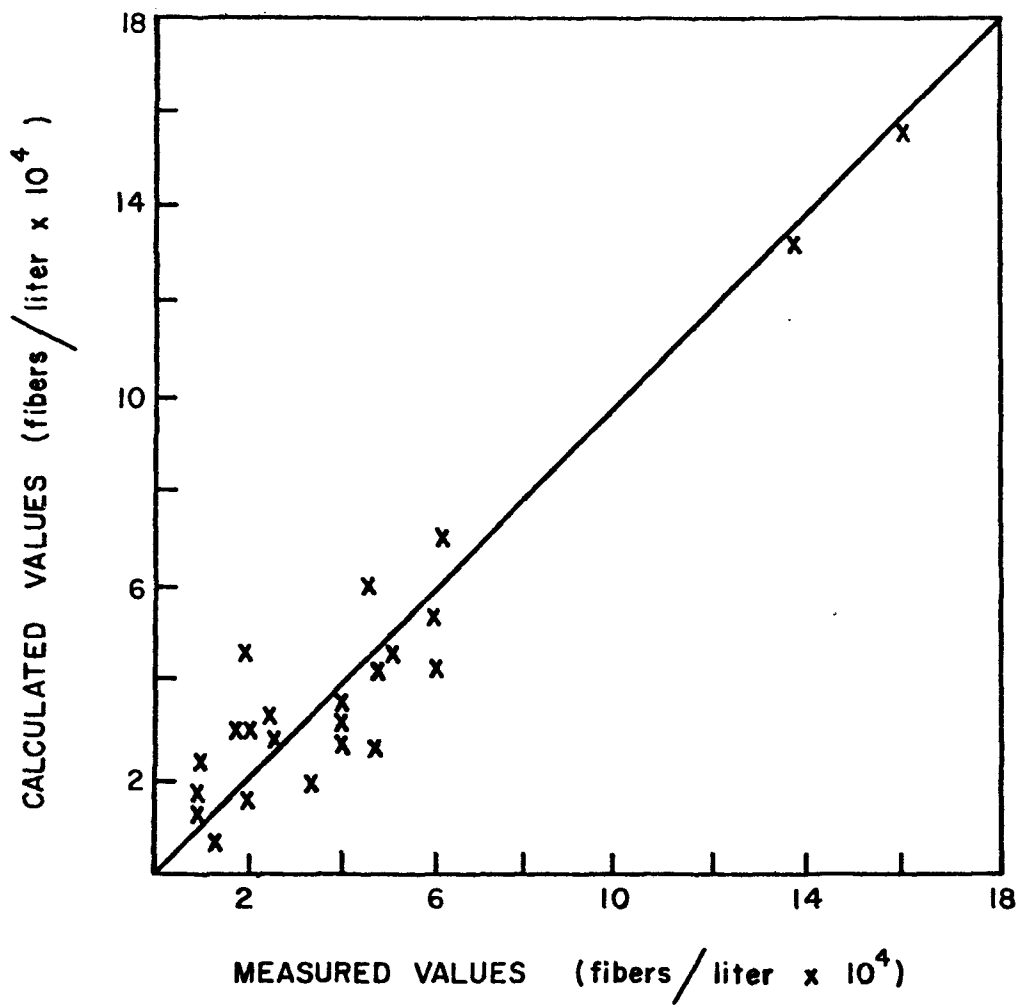


Figure 20. Prediction of amphibole fibers versus the EM measurements for the modified apparatus.



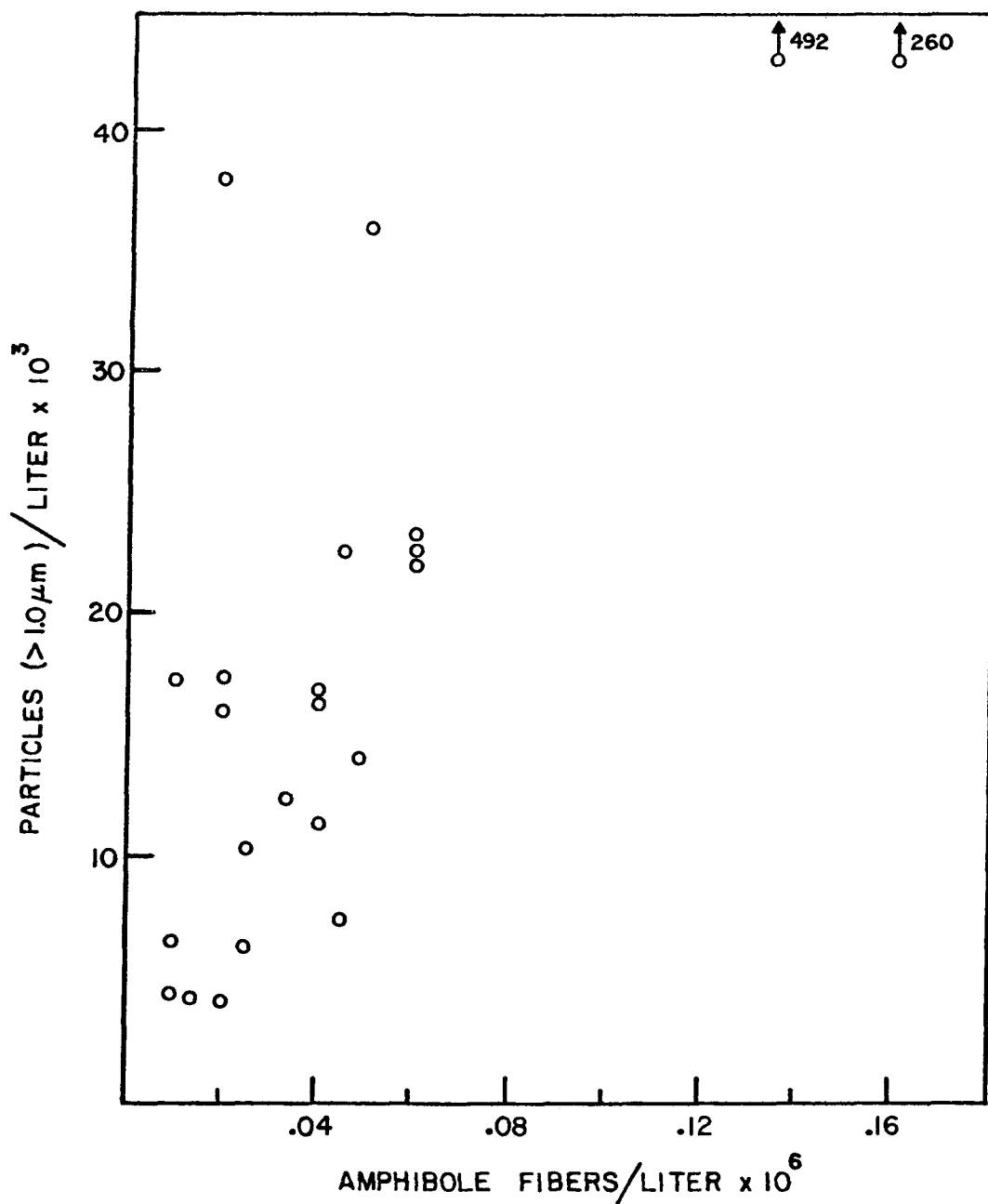


Figure 21. Particle counter data versus EM amphibole fiber counts. (same data as used in amphibole fit of Figure 20)

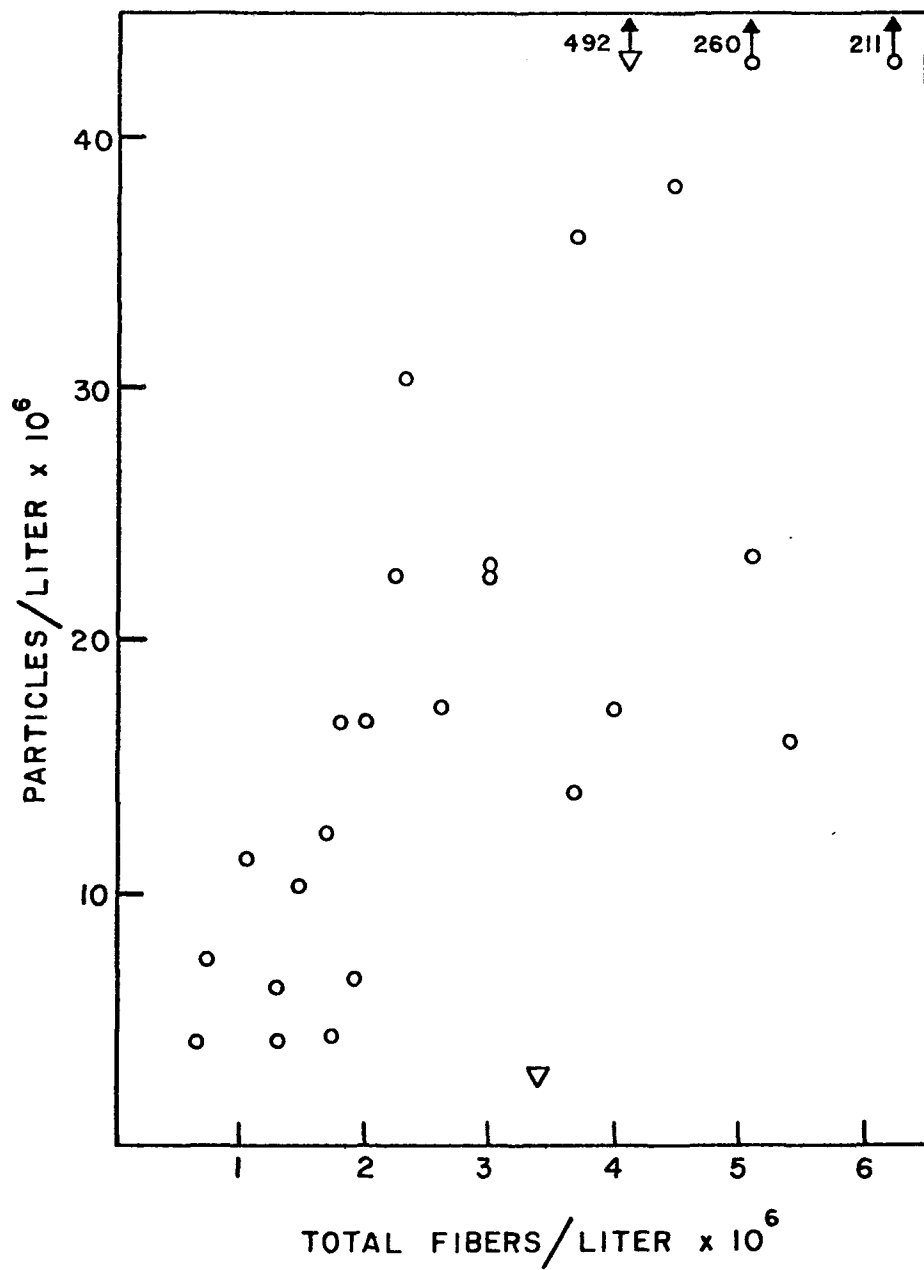


Figure 22. Particle counts versus EM total fiber counts.  
(same data used in 6 variable fit of  
Figure 19)

## REFERENCES

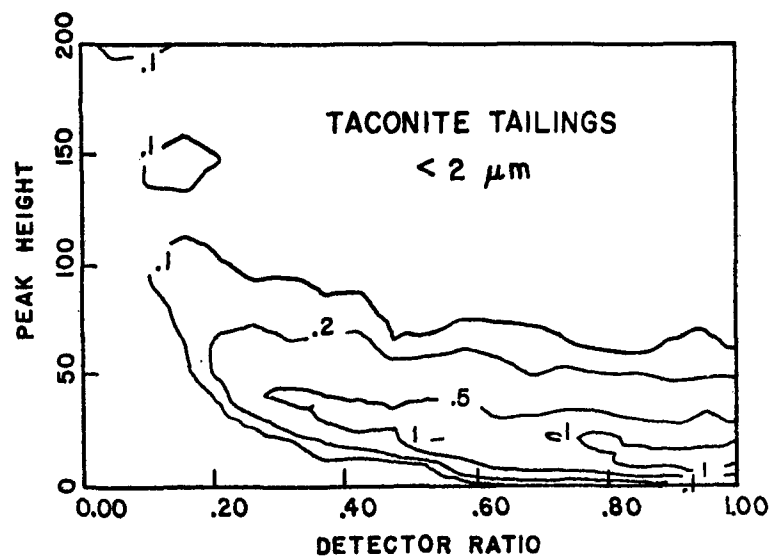
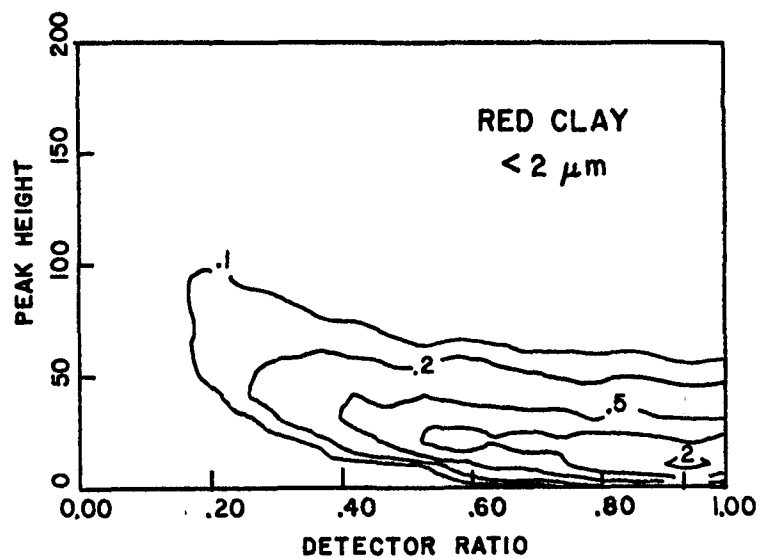
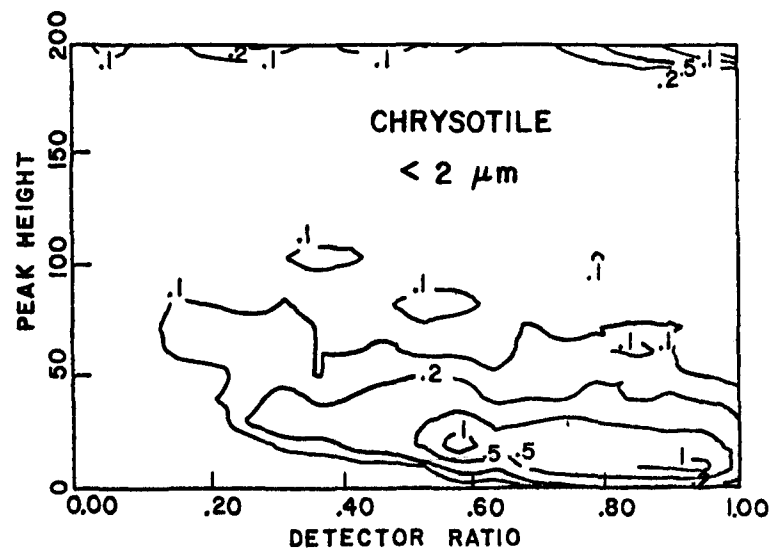
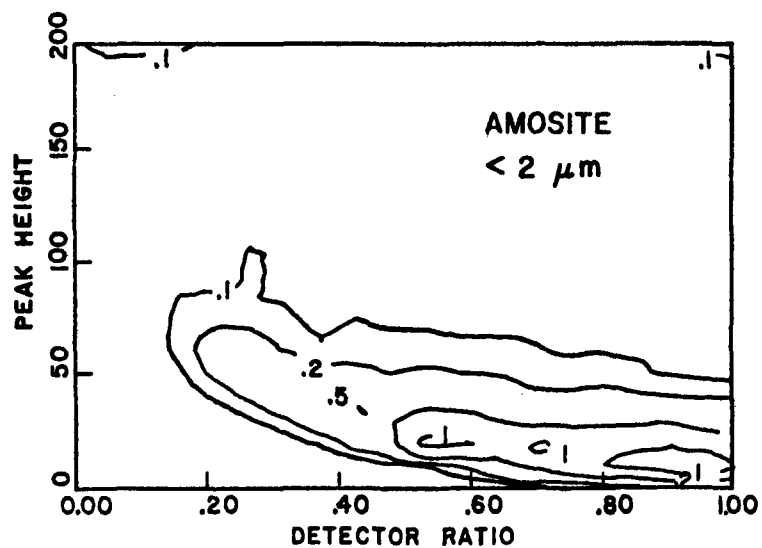
1. Crable, J. V. Determination of Chrysotile, Amosite and Crocidolite by X-ray Diffraction. *Am. Ind. Hygiene Assoc. J.*, 27:293, 1966.
2. Rickards, A. L. Estimation of Trace Amounts of Chrysotile Asbestos by X-ray Diffraction. *Anal. Chem.*, 44:1872, 1972.
3. Rickards, A. L. Estimation of Submicrogram Quantities of Chrysotile Asbestos by Electron Microscopy. *Anal. Chem.*, 45:809, 1973.
4. Leineweber, J. P. Statistics and the Significance of Asbestos Fiber Analysis. Presented at NBS Workshop, Gaithersburg, MD, July 18 - 20, 1977.
5. Rayleigh, Lord. On the Scattering of Light by Small Particles. *Phil. Mag.*, 41, 447-454, 1871.
6. Van de Hulst, H. C. Light Scattering by Small Particles. Wiley Press, New York, 1957.
7. Kerker, M. The Scattering of Light. Academic Press, New York, 1969.
8. Wait, J. R. Electromagnetic Radiation From Cylindrical Structures. Pergamon Press, New York, 1959.
9. Barber, P. and C. Yeh. Scattering of Electromagnetic Waves by Arbitrarily Shaped Dielectric Bodies. *Applied Optics*, 14(22):2864-2872, 1975.
10. Birkhoff, R. D., J. C. Ashley, H. H. Hubbel Jr., and L. C. Emerson. Light Scattering From Micron-Size Fibers. *J. Opt. Soc. Am.*, 67(4):564-569, 1977.
11. Born, M. and E. Wolf. Principles of Optics. Pergamon Press, New York, 1964.
12. Farone, W. A. and M. Kerker. Light Scattering From Long Submicron Glass Cylinders at Normal Incidence. *J. Opt. Soc. Am.*, 56(4):481-487, 1966.
13. Kerker, M., D. Cooke, W. A. Farone, and R. A. Jacobsen. Electromagnetic Scattering From an Infinite Circular Cylinder at Oblique Incidence. *J. Opt. Soc. Am.*, 56(4):487-491, 1966.

14. Gibbs, R. J. Light Scattering From Particles of Different Shapes. J. Geophys. Research, 83(11):501, 1978.
15. Diehl, S. R. and M. Sydor. The Feasibility of Using Optical Methods for the Detection of Asbestos and Red Clay Particles in Lake Superior Water. Mimeo, U.M.D. Dept. of Physics, Duluth, MN, 1975. 42 pp.

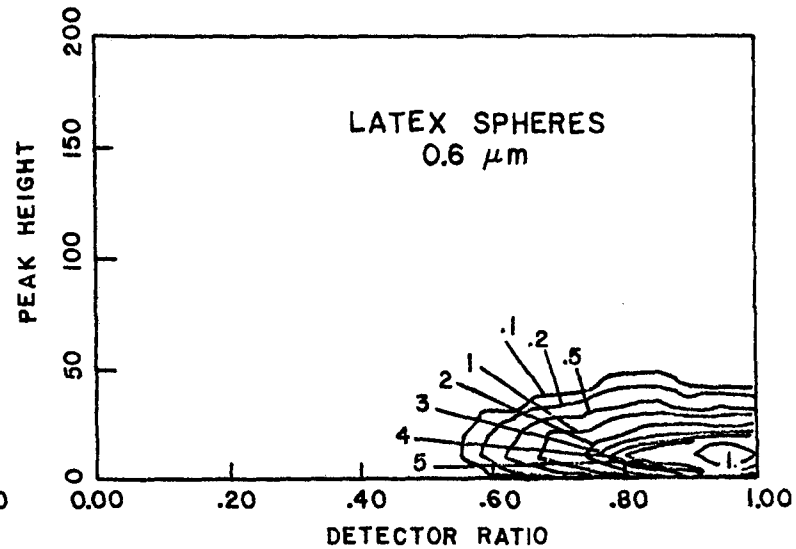
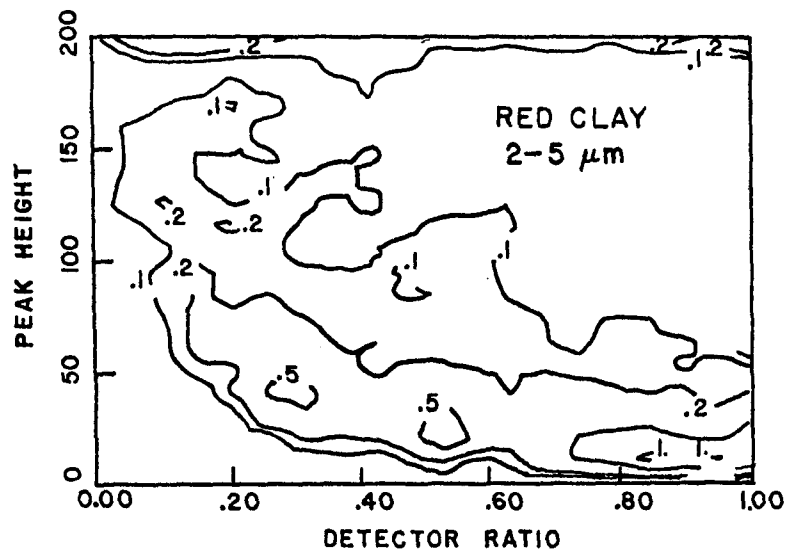
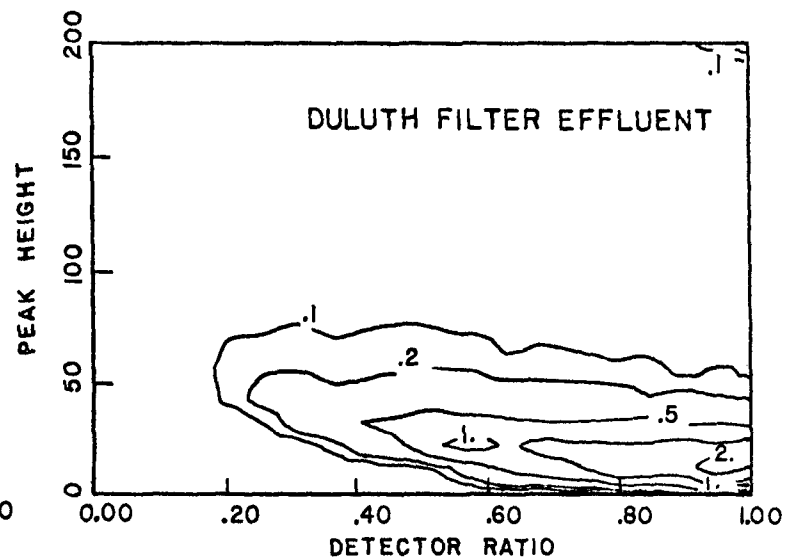
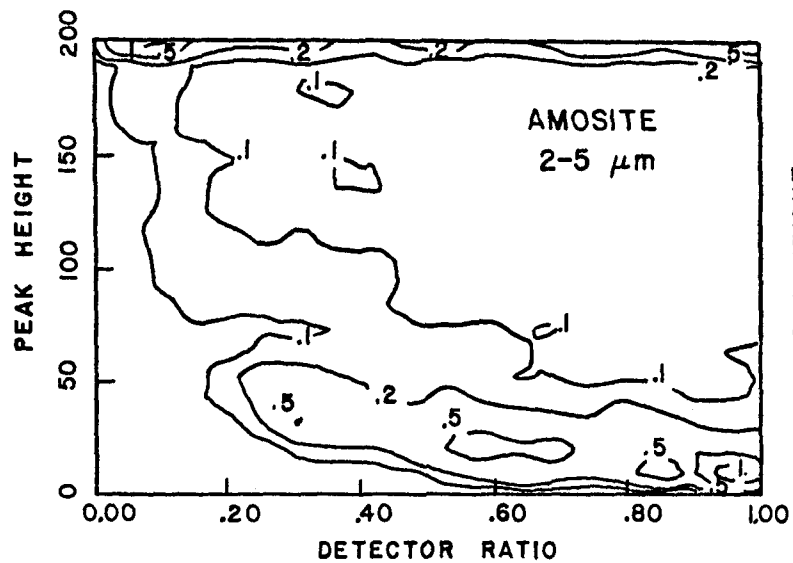
## APPENDIX

### CONTOUR PLOTS OF VARIOUS PARTICLE TYPES

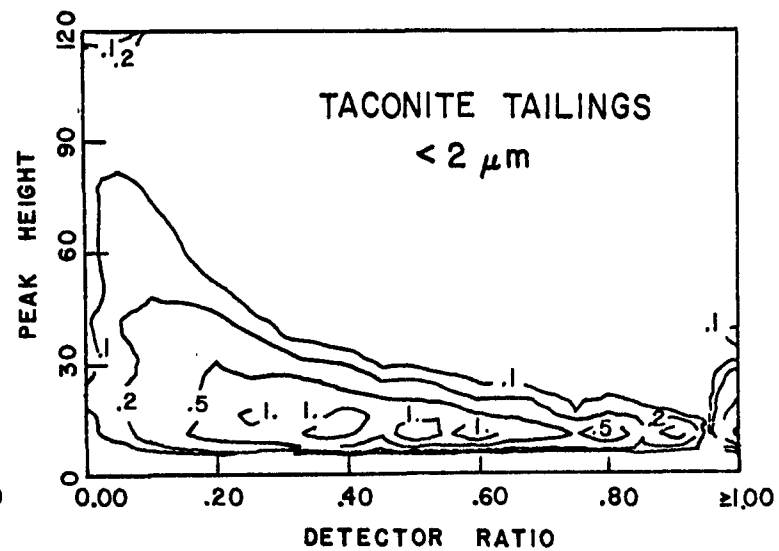
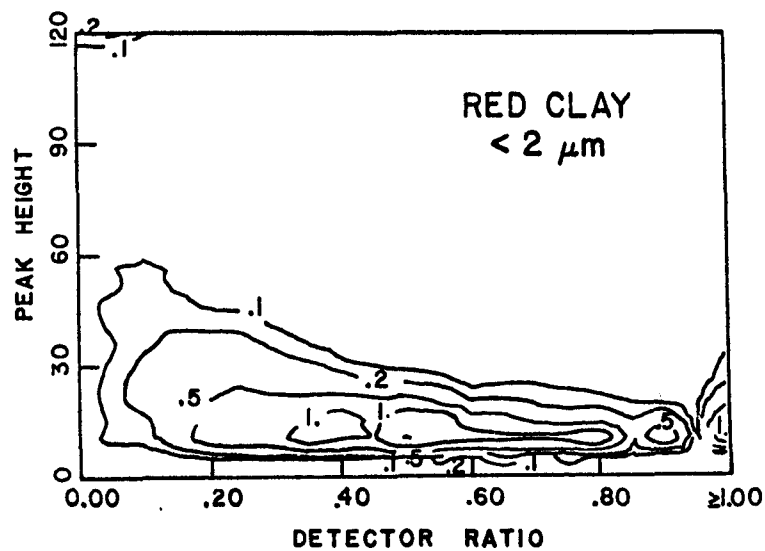
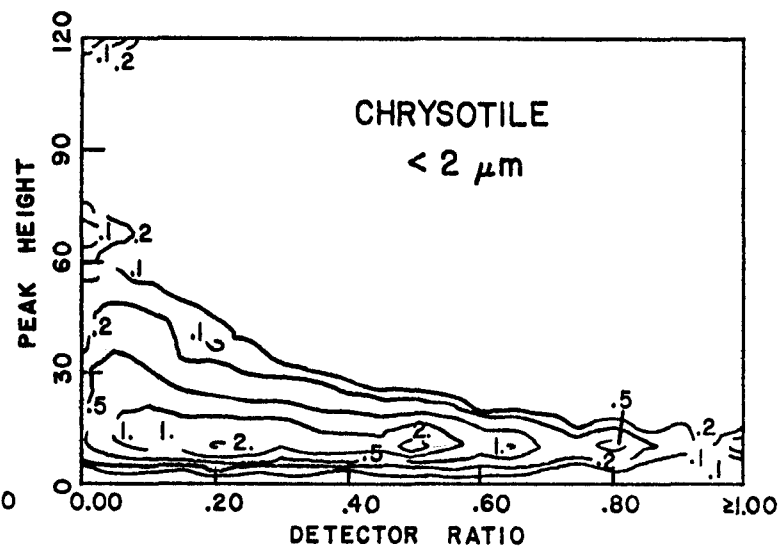
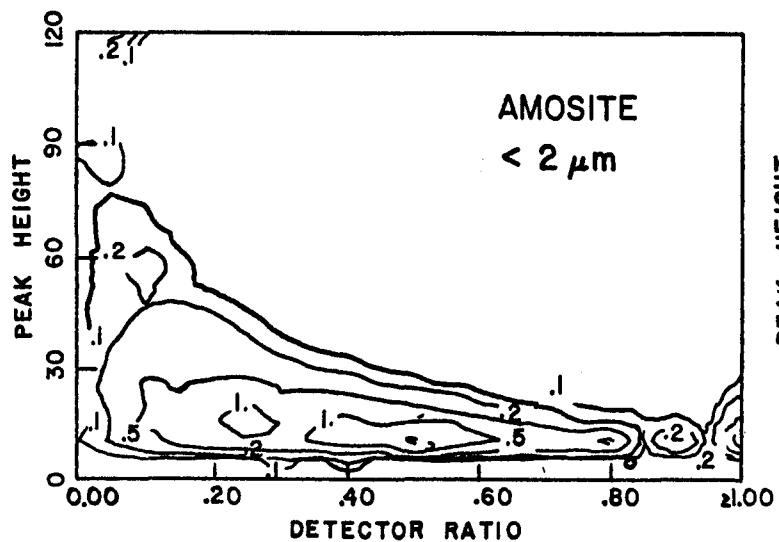
The following are contour plots of the pulse height versus ratio or pulse height versus pulse height arrays for the  $\pm 45^\circ$  and  $+45^\circ, -135^\circ$  detector pairs respectively. The plots were made for each particle species tested by smoothing and normalizing the pulse height arrays and then connecting equal event rates to give lines of equal event probability in percent. These figures can thus be viewed as 3-dimensional frequency plots showing the differences in scattering signatures of the various particle species.



A1. Contour plots of coincident events at the  $\pm 45^\circ$  detectors for the different particle types investigated.

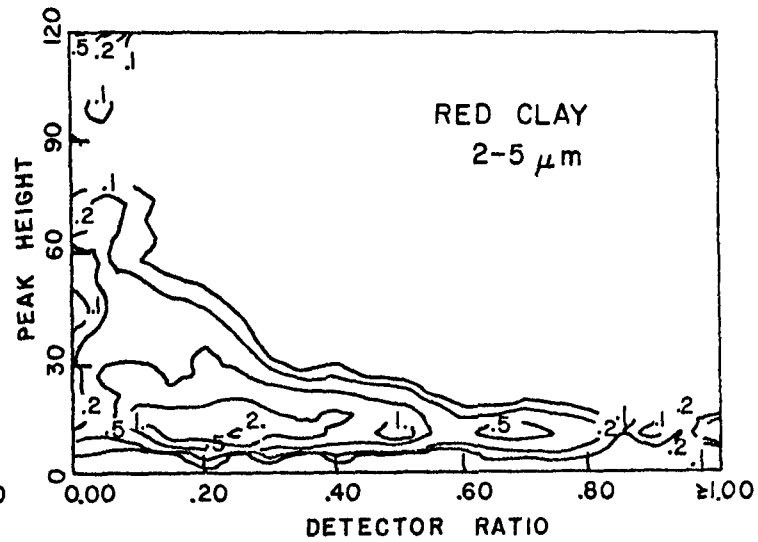
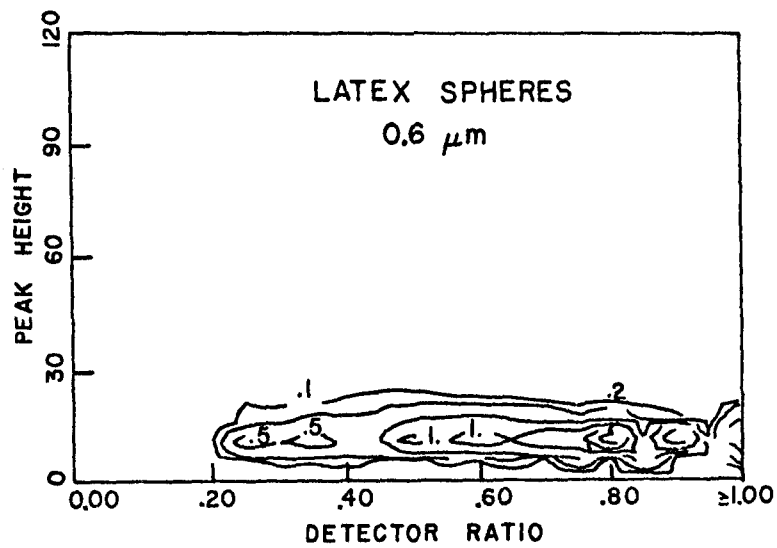
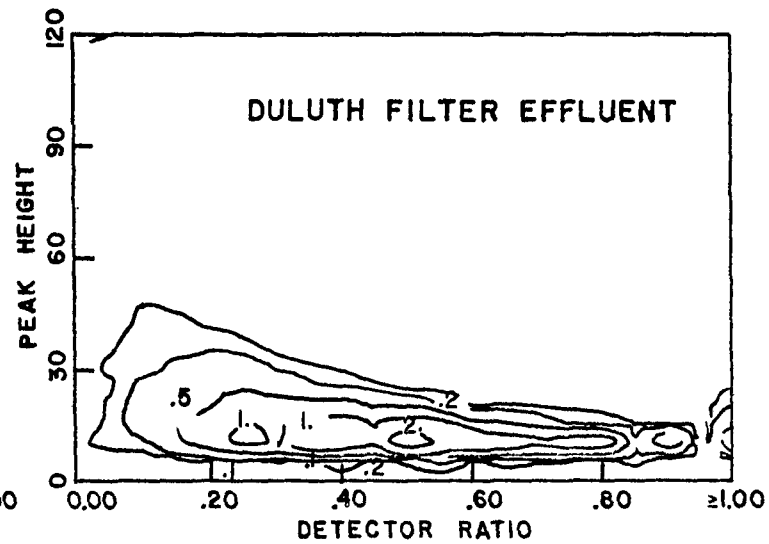
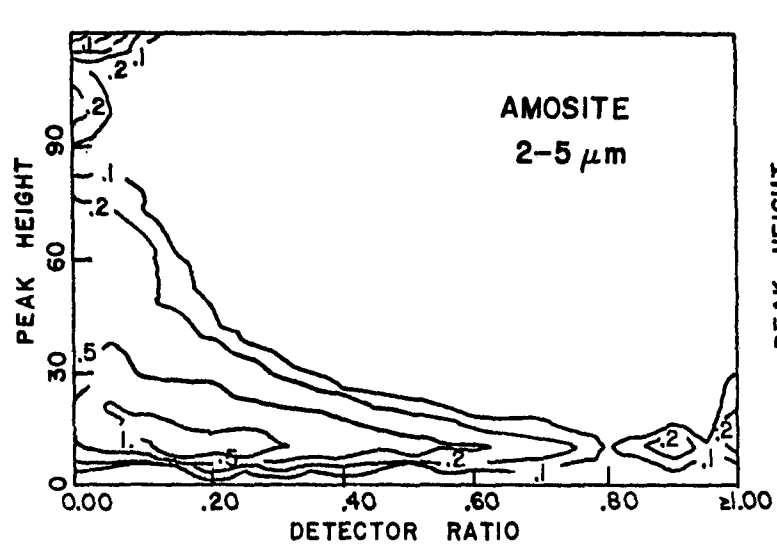


A1. continued

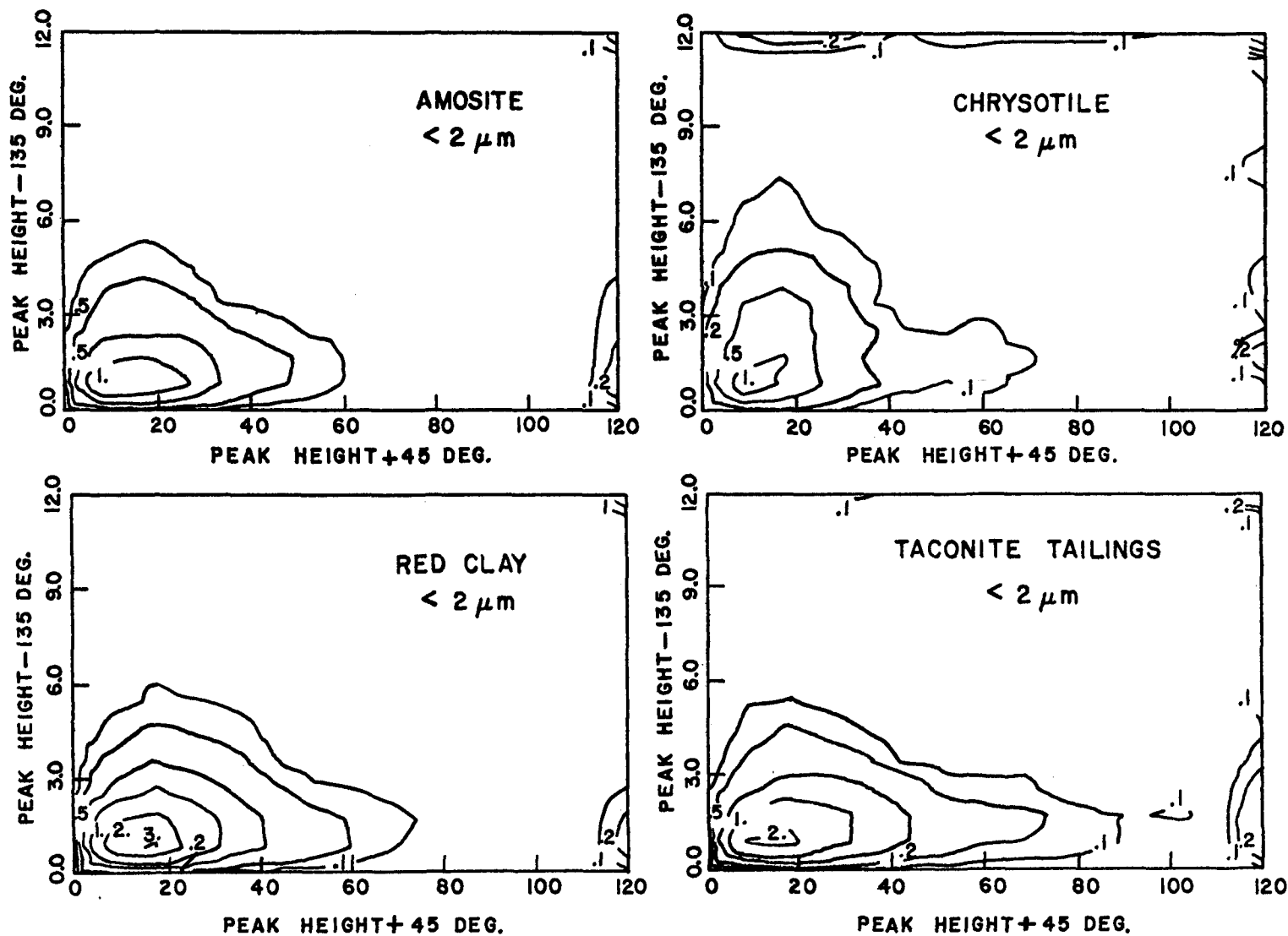


A2. Contour plots of non-coincident events recorded at the  $\pm 45^\circ$  detectors for the different particle types investigated.

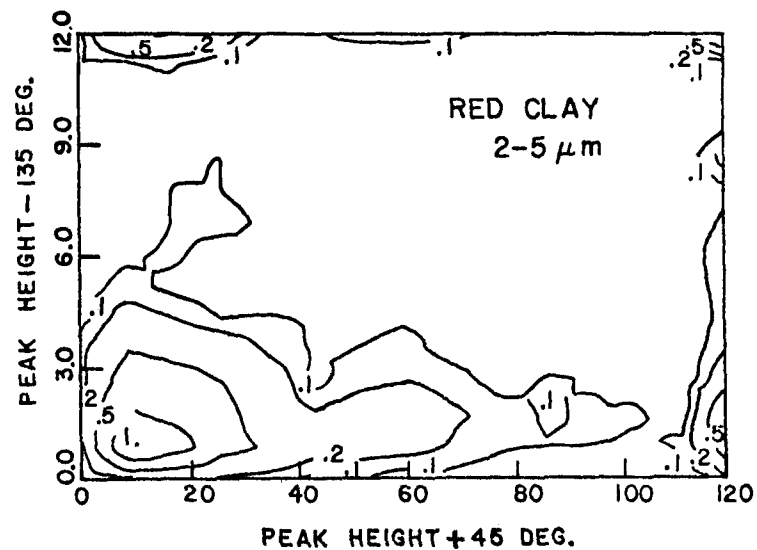
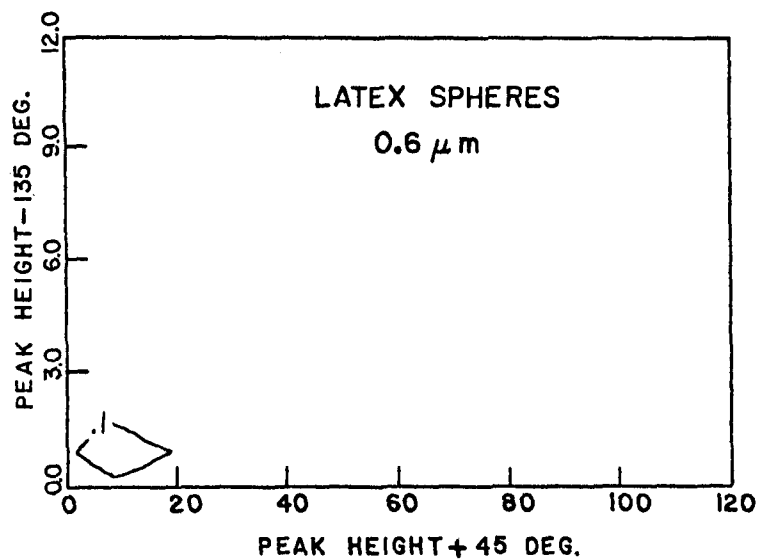
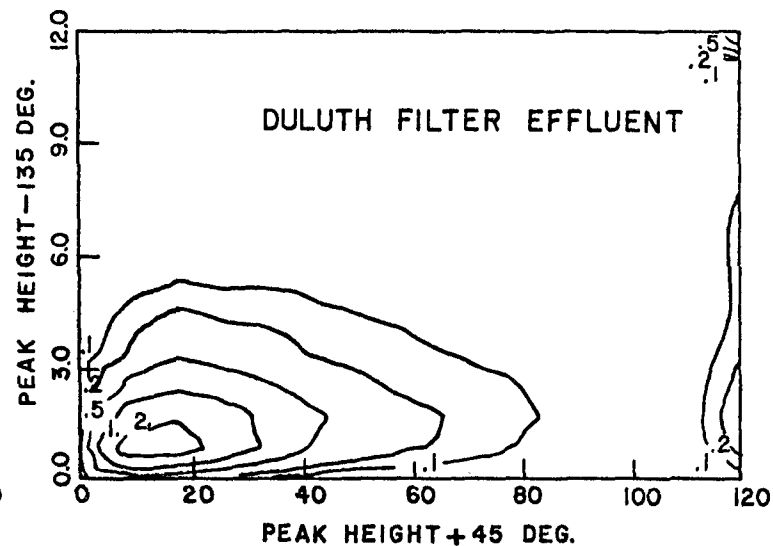
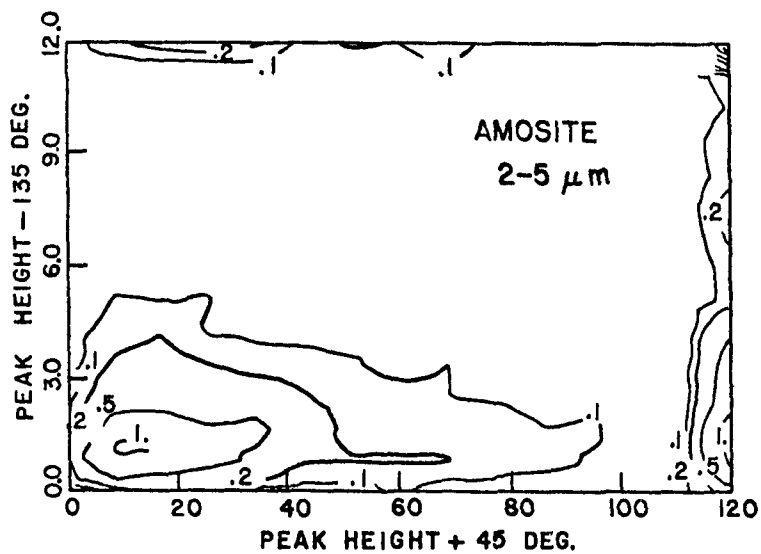




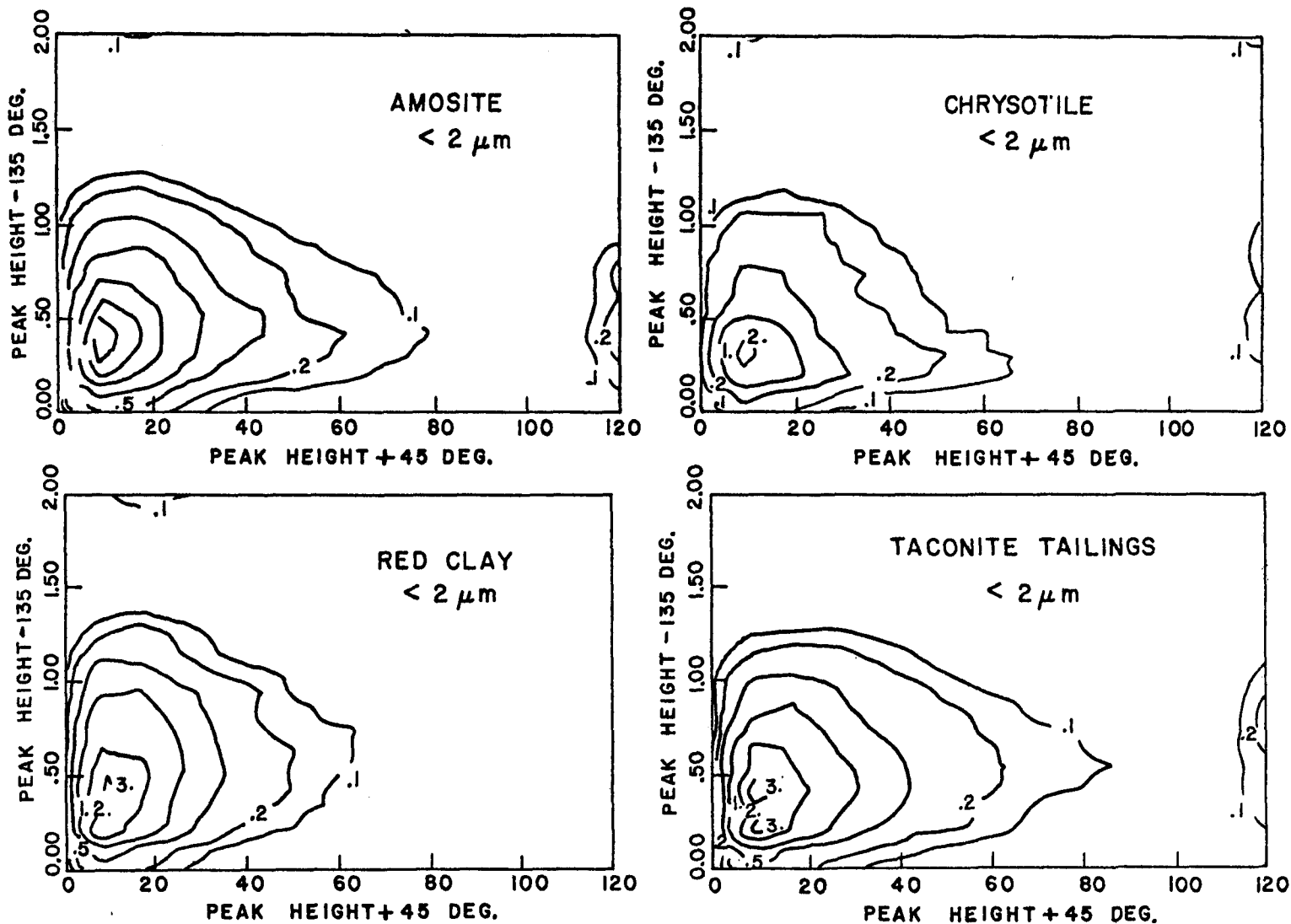
A2. continued



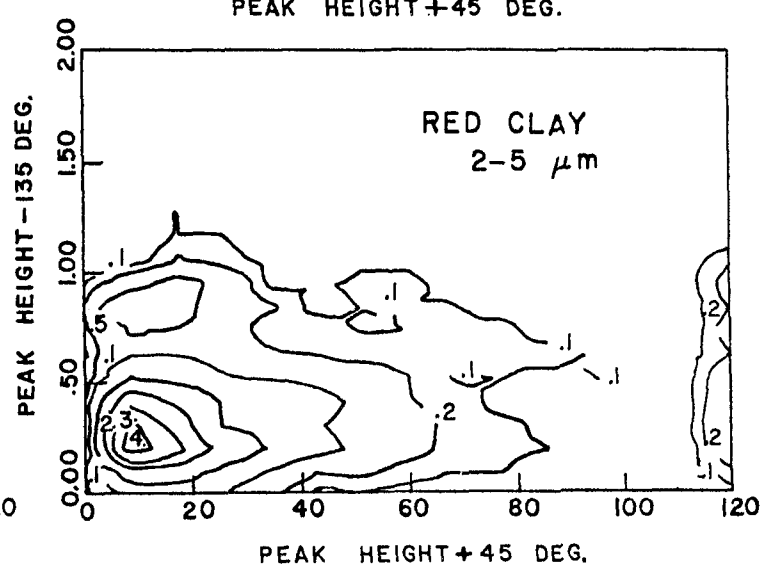
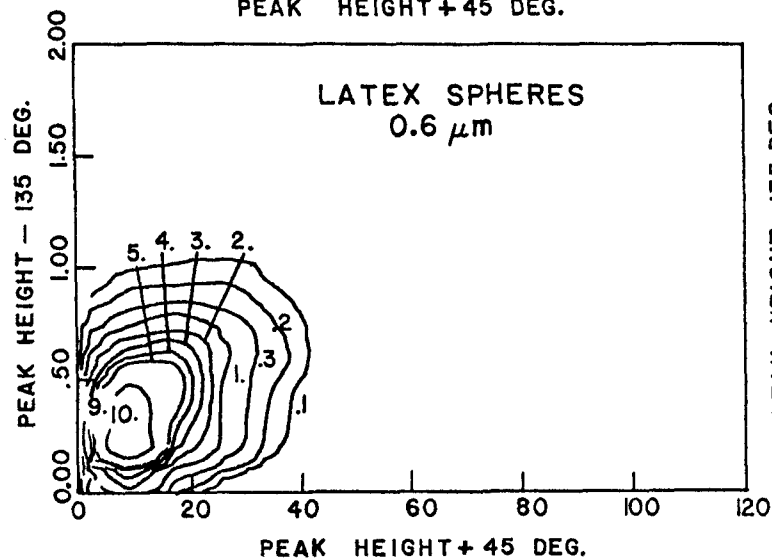
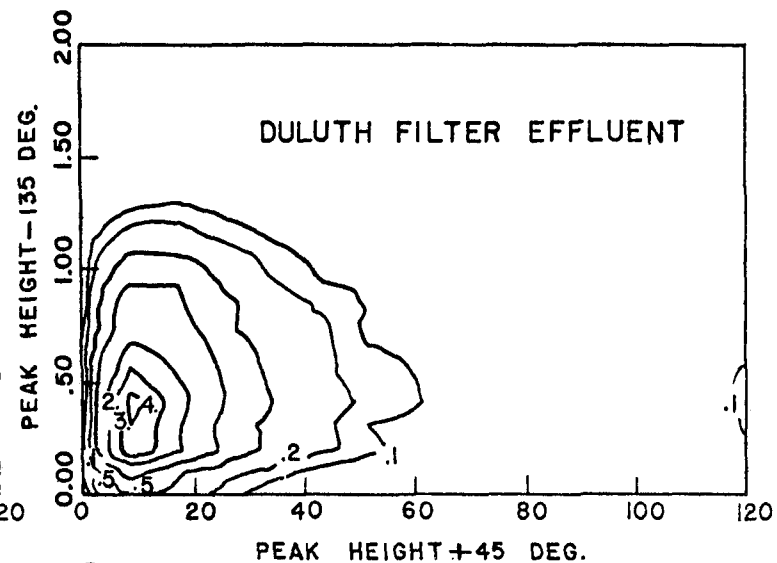
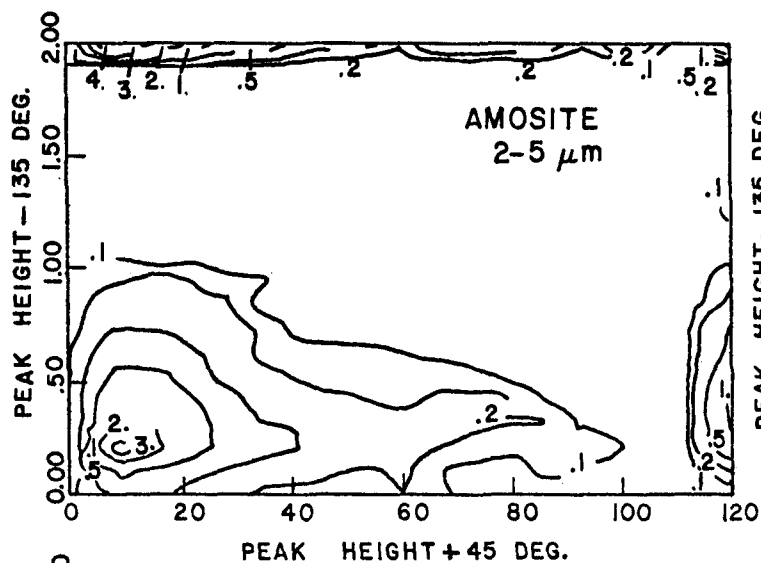
A3. Contour plots of coincident events recorded at the + 45°, - 135° detectors for the different particle types investigated.



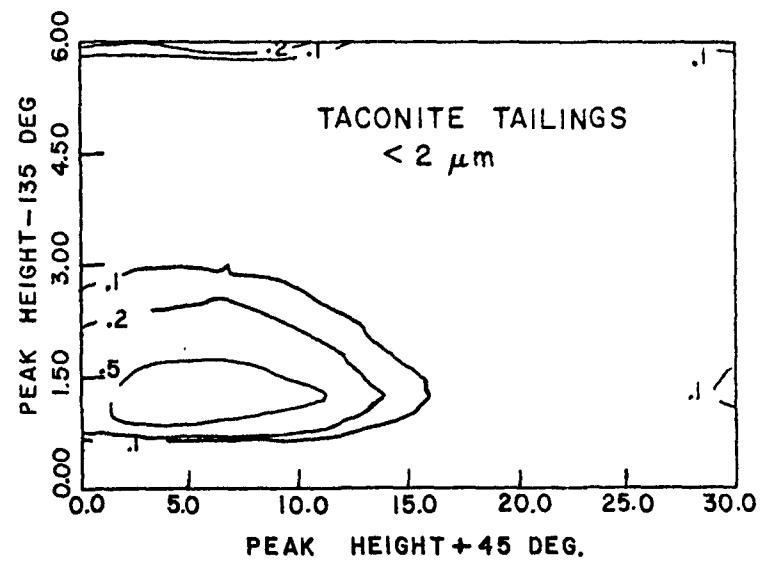
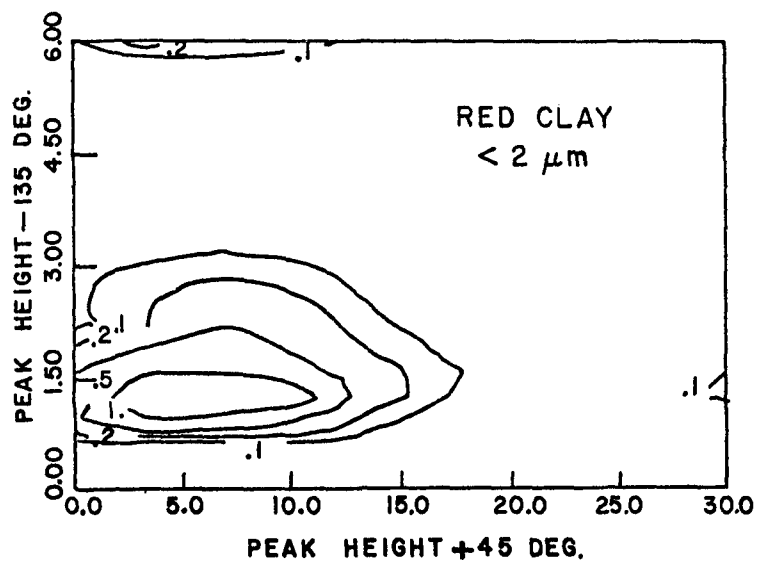
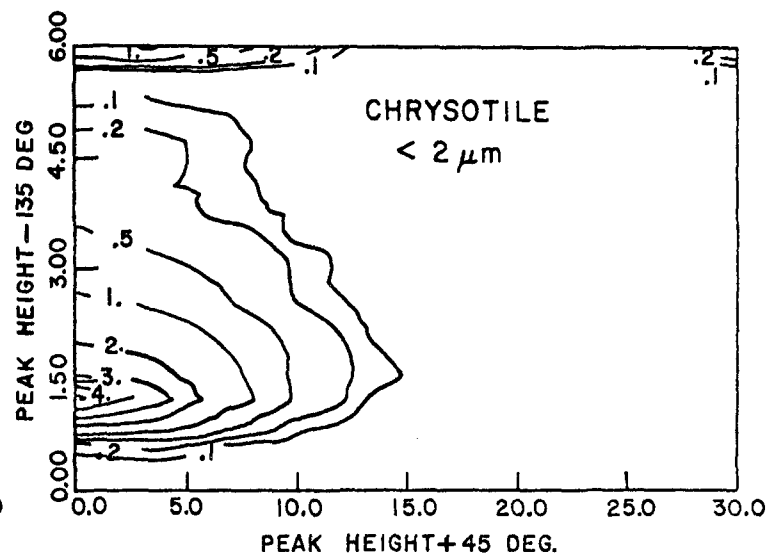
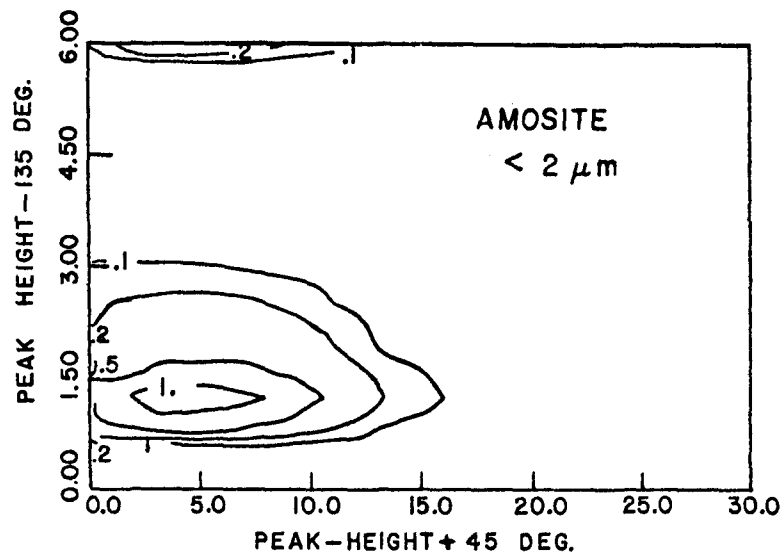
A3. continued



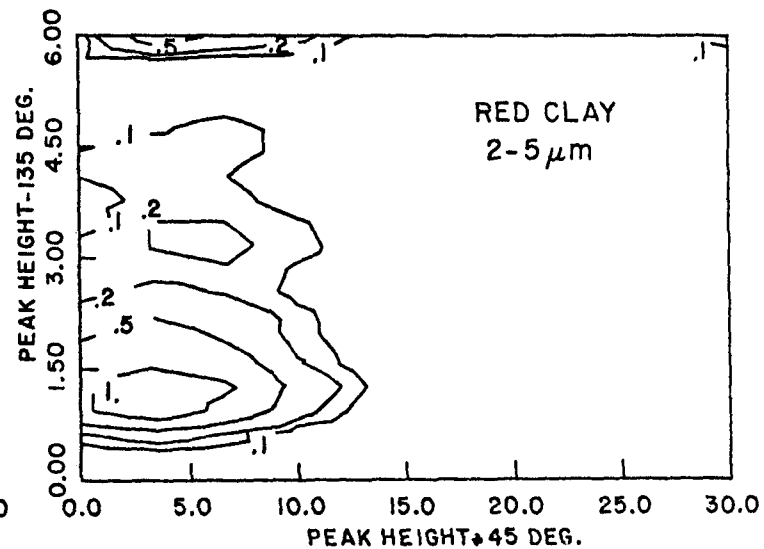
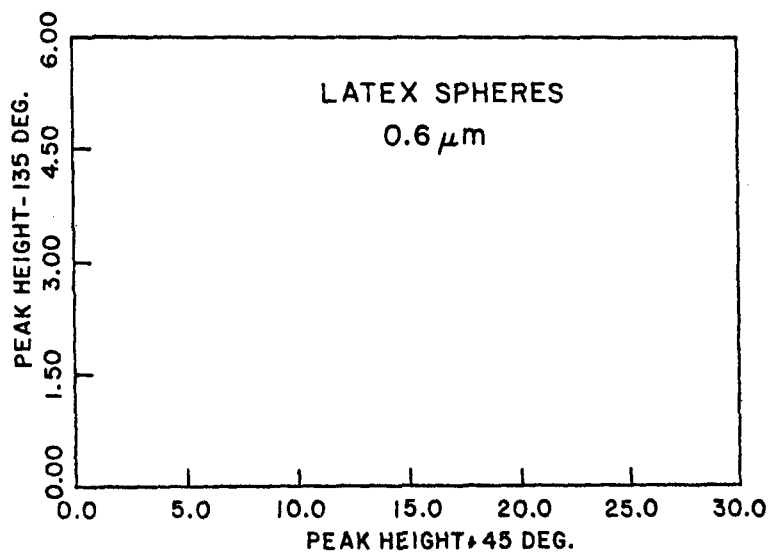
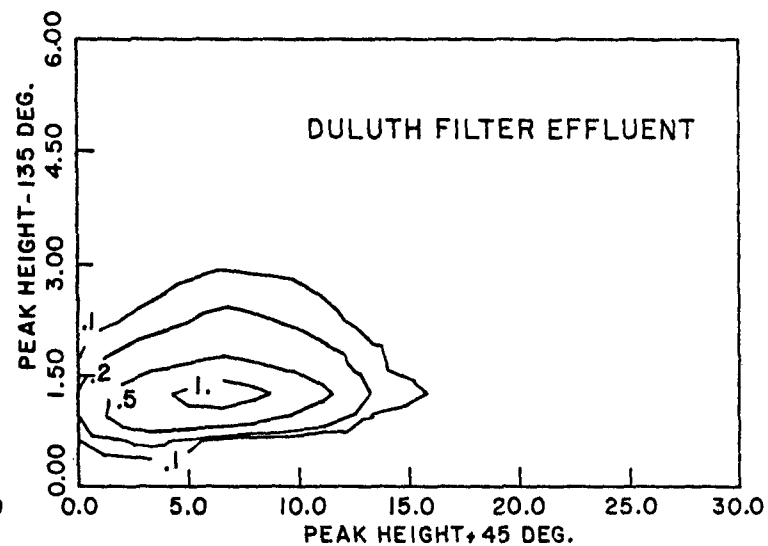
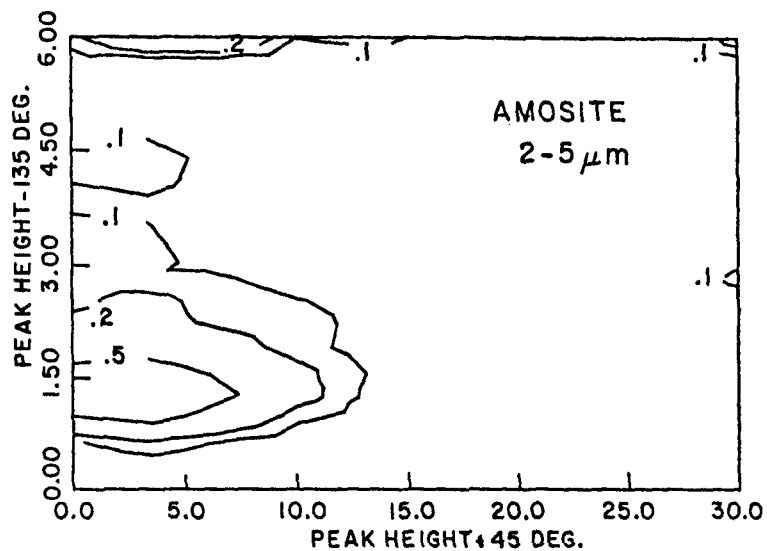
A4. Contour plots of events non-coincident at  $45^\circ$  for the  $+45^\circ$ ,  $-135^\circ$  detectors.



A4. continued.



A5. Contour plots of events non-coincident at  $-135^\circ$  for the  $+45^\circ$ ,  $-135^\circ$  detector pair.



A5. continued

**TECHNICAL REPORT DATA**  
(Please read Instructions on the reverse before completing)

1. REPORT NO. EPA-600/2-79-127		2.		3. RECIPIENT'S ACCESSION NO.	
4. TITLE AND SUBTITLE Optical Detection of Fiber Particles in Water				5. REPORT DATE August 1979 (Issuing Date)	
				6. PERFORMING ORGANIZATION CODE	
7. AUTHOR(S) S.R. Diehl, D.T. Smith, M. Sydor				8. PERFORMING ORGANIZATION REPORT NO.	
9. PERFORMING ORGANIZATION NAME AND ADDRESS Department of Physics University of Minnesota, Duluth Duluth, Minnesota 55812				10. PROGRAM ELEMENT NO. 1CC614 SOS 1 Task 07	
				11. CONTRACT/GRANT NO. R804361	
12. SPONSORING AGENCY NAME AND ADDRESS Municipal Environmental Research Laboratory--Cin., OH Office of Research & Development U.S. Environmental Protection Agency Cincinnati, Ohio 45268				13. TYPE OF REPORT AND PERIOD COVERED Final 3/76 - 9/78	
				14. SPONSORING AGENCY CODE EPA/600/14	
15. SUPPLEMENTARY NOTES Project Officer: Gary S. Logsdon (513) 684-7345					
16. ABSTRACT  Light scattering by individual particulates is used in a multiple-detector system to categorize the composition of suspended solids in terms of broad particulate categories. The scattering signatures of red clay and taconite tailings, the two primary particulate contaminants in western Lake Superior, along with two types of asbestiform fibers, amphibole, and chrysotile, were studied in detail. A method was developed to predict the concentration of asbestiform fibers in filtration plant samples for which electron microscope analysis was done concurrently. Fiber levels as low as $5 \times 10^4$ fibers/liter were optically detectable. The method offers a fast and inexpensive means for measuring, either on a continuous basis or as discrete samples, the fiber levels of filtration plant output. Further calibration of the instrument could enable analysis for other specific particulate contaminants as well.					
17. KEY WORDS AND DOCUMENT ANALYSIS					
a. DESCRIPTORS		b. IDENTIFIERS/OPEN ENDED TERMS		c. COSATI Field/Group	
amphiboles, asbestos, clays, colloids, detectors, fibers, light (visible radiation), optical detection, particle shape, water		light scattering, taconite tailings, red clay, Lake Superior, chrysotile particle detector		20 F	
18. DISTRIBUTION STATEMENT RELEASE TO PUBLIC		19. SECURITY CLASS (This Report) UNCLASSIFIED		21. NO. OF PAGES 71	
		20. SECURITY CLASS (This page) UNCLASSIFIED		22. PRICE	